

Modelling the transport of organic matter over tidal sand waves

**UNIVERSITY
OF TWENTE.**

Master thesis

Arjan van den Broek

Enschede, April 2019



Royal Netherlands Institute
for Sea Research

Modelling the transport of organic matter over tidal sand waves

Master thesis

Water Engineering & Management
Faculty of Engineering Technology
University of Twente

April, 2019

Author: J. (Arjan) van den Broek
Location: Enschede and Yerseke
Organization: University of Twente & Royal
Netherlands Institute for Sea
Research (NIOZ)

Graduation committee:

University of Twente
Ir. J.H. Damveld
Dr. Ir. B.W. Borsje
Prof. Dr. S.J.M.H. Hulscher
NIOZ
C. Cheng, MSc
Prof. Dr. K. Soetaert

Preface

This report is the result of my master thesis project about '*Modelling the transport of organic matter over sand waves*', which is the final project of the Master Water Engineering & Management at the University of Twente. The master thesis is executed at the Royal Netherlands Institute of Sea Research (NIOZ) and the University of Twente.

I would like to thank my supervisors, with Johan Damveld in particular for the weekly support, his revisions during the study and his suggestions on structuring the report. Also, Bas Borsje for giving me the opportunity to start research on this topic and to present my results at the NCK days 2019. Suzanne Hulscher for her suggestions on the report and the trust towards the end of the process. Furthermore, I would like to thank Karline Soetaert, who helped me a lot by informing me about using the biogeochemical model. Finally, I would like to thank Chiu Cheng for his help during my stay in Yerseke, his guidance during the study and the useful feedback regarding my English language.

Arjan van den Broek
April, 2019

Abstract

The bed of shallow shelf seas such as the North Sea consists of sand waves and is a habitat for benthic organisms, as these two have an influence on each other. Sand waves are rhythmic bedforms of several meters high, have wavelengths of hundreds of meters and migrate several meters per year. A hydro-morphological model in Delft3D has been made to predict the behaviour of the sand waves. The presence of benthic organisms can also change the characteristics of the sediment and consequently the sediment transport. To understand how the benthic organisms affect the sand wave dynamics, it is necessary to first characterize the food-supply of these benthic organisms. A biogeochemical model using organic matter and flow velocity to determine where the organic matter will settle down was applied, in which the organic matter is used as a proxy for food for the benthic organisms. Thus the organic matter could provide a preliminary prediction on the distribution of the benthic organisms along the sand waves. Nevertheless, existing research about the connection between hydrodynamics and ecology is scarce. A one-way coupling between the models will give insight in the transport of organic matter over sand waves. Therefore, this research connected the hydro-morphological model with the biogeochemical model.

The coupling between the two models is a one-way coupling in which the hydrodynamics of the hydro-morphological model (e.g. horizontal and vertical flow velocity and vertical diffusivity) has been used as input in the biogeochemical model. The inputs from the hydro-morphological model differ in bathymetry and forcing conditions, i.e. tidal symmetry and residual currents. Together with the organic matter and several processes in the biogeochemical model (e.g. advection, dispersion, sinking and respiration), the one-way coupling is able to predict the distribution of the organic matter over the different sand waves. The bathymetry and forcing condition have an influence on the organic matter concentration over the sand waves. The tide-averaged organic matter concentration shows higher concentrations just above the trough on both sides of the symmetrical sand wave and only on the lee side of the asymmetrical sand wave. Furthermore, the results show two behaviours during one tidal cycle of twelve hours. Namely, an increase in organic matter concentration during flood and ebb tide just above the troughs and an uni-directional organic matter transport during slack tide. During flood and ebb tide instantaneous circulations occur, which causes the increase in organic matter concentration. During slack tide, there is almost no flow and the organic matter concentration in the water column will be transported by the tidal reversal. Here, the results showed that the transport is over at least three sand waves. This research concludes that the highest organic matter concentration are found just above the trough and the one-way coupling of the two models generates a more accurate prediction of that.

In conclusion, this research calls for a further extension on the two models, as a two-way coupling could determine the distribution of the different benthic organisms depending on how they capture their food. Furthermore, the interaction between the sand wave dynamics and the benthic organisms could then be predicted.

Contents

1. Introduction.....	11
1.1 Problem definition.....	11
1.2 Knowledge gap	13
1.3 Research objective	14
1.4 Method.....	14
1.5 Outline	15
2. Theoretical concepts	16
2.1 Hydro-morphological model realisation	16
2.2 Delft3D.....	16
2.3 Marine ecology.....	17
2.4 Organic matter	17
2.5 Biogeochemical model	17
2.6 Site Texel	17
3. Model description	19
3.1 Hydro-morphological model	19
3.1.1 Hydrodynamic equations	19
3.1.2 Sediment transport and bed evolution	20
3.1.3 Model set-up	20
3.2 Biogeochemical model	22
3.2.1 Processes	23
3.2.2 Model set-up	24
3.2.3 Assumptions	26
3.3 Grid.....	26
4. Results	27
4.1 General	27
4.2 Hydrodynamics.....	27
4.2.1 Flow velocity.....	27
4.2.2 Near-bed velocity	29
4.2.3 Vertical velocity	29
4.2.4 Diffusivity.....	30
4.2.5 Slack tide.....	31
4.3 Organic matter	33

4.3.1 Tide-averaged.....	33
4.3.2 Organic matter over time.....	33
4.3.3 Lee side of the asymmetrical sand wave.....	35
4.4 Texel	36
4.4.1 Tide-averaged.....	36
4.4.2 Wave height.....	37
4.5 Physical explanation.....	37
5. Discussion.....	39
6. Conclusion and recommendations.....	42
6.1 Conclusion	42
6.2 Recommendations.....	44
References.....	45

Introduction

Across the sea there are various bed patterns, ranging from small ripples to large sand banks, of which sand waves are the most dynamic. Sand waves can be dynamically active and show displacement rates of up to tens of meters per year (Terwindt, 1971). The profile of the sand wave is symmetric unless either significant residual currents are present, or the tidal wave is asymmetric (Besio et al., 2006). To understand the behaviour of sand waves, a numerical hydro-morphological model was made in Delft3D (van Gerwen et al., 2018).

The bottom of the North Sea consists of a diverse community of benthic organisms, some of which have the ability to change the characteristics of the sediment and consequently, the sediment transport. This can also have an influence on the dynamics of the sand waves. For example, some studies have shown a difference in benthic assemblage along the sand waves (e.g. Baptist et al., 2006; Damveld et al., 2018). However, the sampling and characterization of the benthic community, and measurements of hydrological processes under natural conditions in general, are often difficult due to methodological limitations (Janssen et al., 2012). Thus, the distribution of organic matter over sand waves could be used as a proxy for the first indication of the potential types of benthic organisms that may be found. This can be predicted by the biogeochemical model (Soetaert et al., 2016).

A coupling between these two models will give more insights in the distribution of the organic matter along the sand wave.

1.1 Problem definition

Coastal areas are highly important both from an ecological and economical perspective (Borsje et al., 2009). Predictions of sand wave dynamics are important for several offshore activities, including pipelines, wind farms, shipping lanes and buried objects (Németh et al., 2003). This would lead to cost reductions for example. Similarly, predictions on the distribution and the behaviour of benthic organisms are important for the ecology, as they create and maintain their surrounding habitat.

Over the years several studies have been carried out to investigate the behaviour of sand waves. Stability analysis is often used to predict the morphological features and seabed dynamics. Both linear and non-linear models are used to forecast the sand wave dynamics. Hulscher (1996) started with modelling the sand wave growth using Linear Stability Analysis (LSA). Following this study, several extensions have been made such as the migration (Besio et al., 2004; Németh et al., 2002), benthic organisms (Borsje et al., 2009; Maris, 2018) or physical mechanisms including grain size variation (Roos et al., 2007). Some of these studies were based on LSA, but as amplitudes increase, the non-linear effects become important. With the non-linear models, a hydro-morphological model is created with the help of the process-based model Delft3D, which models sand waves from its initial stage until an equilibrium is achieved (van Gerwen et al., 2018). In this study, they used two types of sand waves, a symmetrical and an asymmetrical sand wave, with a difference in bathymetry and forcing conditions. Both had a symmetrical tide, but only the asymmetrical sand wave had a residual current. Compared to LSA, many physical processes, such as wind- and wave driven current and sediment transport can be included and Delft3D holds for large amplitudes.

The bed of the North Sea is often covered by a diverse assemblage of benthic organisms. They can have a large effect on the sediment dynamics in shallow coastal seas (Widdows & Brinsley, 2002). Thus, it is believed that these animals can also influence the sand wave dynamics. Some benthic organisms will hold sediment by creating a patch of tube structures or other protrusions (Maris, 2018), which could slow down the migration of the sand wave, or loosen up the bed by digging, which can make the sediment more prone to erosion, and thereby increase the migration. To better understand how the benthic organisms affect the seabed, it is fundamental to characterise their structural and dynamic response to the quantity, quality and timing of food supply (Lessin et al., 2019). A study by Shimeta, (2009) suggests that the flow velocity has an influence on the growth and population dynamics of the benthic organisms. Shimeta (2009) compared the functional response of *Polydora cornuta* (a tube-building polychaete) at different flow velocities and determined whether food capture was proportional to particle flux (concentration * velocity). The quality of organic matter that becomes incorporated in the sediment concentration is also an important characteristic of a benthic system, because of benthic fluxes and carbon mineralization (Soetaert et al., 1996). The rate of mineralization can be an indication of the amount of organic matter, which is a food source for the benthic organisms, as well as the level of biological activity occurring in the sediment.

Maris (2018) showed with Delft3D that the benthic organism *Lanice conchilega* is able to change the hydrodynamics and consequently the sediment dynamics. Moreover, this study showed a difference in the benthic assemblage over the sand waves, which also was observed in field studies (e.g. De Jong et al., 2015). More recently, data was collected from two field campaigns in a sand wave field in the Dutch North Sea, near Texel. The results of this field campaign showed a higher abundance in both epi- and endobenthos in the sand wave troughs compared to the crests (Damveld et al., 2018) as well as a difference in sediment sorting and permeability over the sand waves (Cheng et al., submitted). However, the model in Maris (2018) has a shortcoming in terms of implementing the sediment as a food source. Here, the suspended sediment is used as the available food for the worms. Two restrictions are made to increase the density, but in the troughs the density becomes smaller than half-way the flanks. In addition, the model uses one grain size, while in reality the troughs of the sand waves consists of finer-grained and less well-sorted sediment (Roos et al., 2007). This means that there is more sediment available as food for the worms (Maris, 2018). Using more grain sizes was not possible due to computational time. This will also be the case when the model has to be run for more benthic organisms, because the North Sea consists of a wide range of benthic organisms instead of the one that is used in the model.

The biogeochemical model can solve the food source problem. This model makes use of organic matter and flow velocity and aims to determine where the organic matter will accumulate or settle down. By using organic matter as a proxy for food for the benthic organisms, this could provide a preliminary prediction on the distribution of the benthic organisms. An explanation can be made by evaluating the interaction between the benthic assemblage and the organic matter concentration over sand waves. Thus far, the biogeochemical model has only been used for coral reefs in oceans (Soetaert et al., 2016). In this study a hydrodynamic model, biogeochemical model and habitat suitability model were coupled to understand the transport of organic matter to cold-water corals (CWCs). Results showed that the interaction between tidal currents and CWCs induces downwelling events of surface water that bring organic matter to CWCs at 600-m depth. Both these carbonate mounds and enhanced food supply are essential for the sustenance of the CWCs.

To understand the distribution of organic matter in a sand wave field, a coupling is needed between the hydro-morphological model and the biogeochemical model. This has never done before and a good understanding between the hydrodynamics and ecology (e.g., benthic organisms) is currently lacking.

This will be done by coupling the hydro-morphological model and the biogeochemical model, in which the distribution of organic matter over sand waves can then be determined, see Figure 2. This could give insights in the interaction between the hydrodynamics and the benthic organisms and could clarify why benthic organisms are found more predominately in the troughs than in the crest (Damveld et al., 2018; Cheng et al., submitted).

1.2 Knowledge gap

It is important to understand the link between the ecological and physical processes. In the past these two were investigated separately, despite the potential influence of benthic organisms and sand waves on each other. Maris (2018) investigated the two-way coupling between sand waves and *L. conchilega*, but in this research suspended sediment was used as food for the worms. Two restrictions are used to increase the density of the sediment along the sand waves. However, in the troughs the density becomes smaller than half-way the flanks, which in reality is not true. Using organic matter as food for the benthic organisms in the context of a sand wave field has never done before, but could solve the food source problem, as seen in Soetaert et al. (2016). Therefore a coupling is needed between a hydro-morphological model and a biogeochemical model.

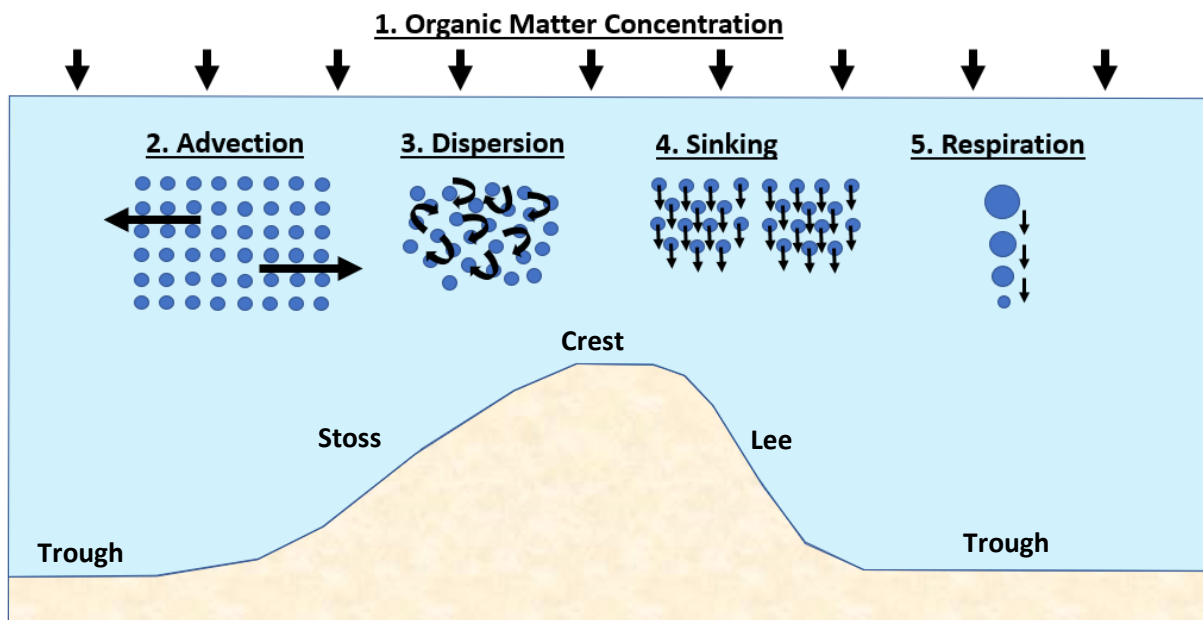


Figure 1 The processes of the biogeochemical model.

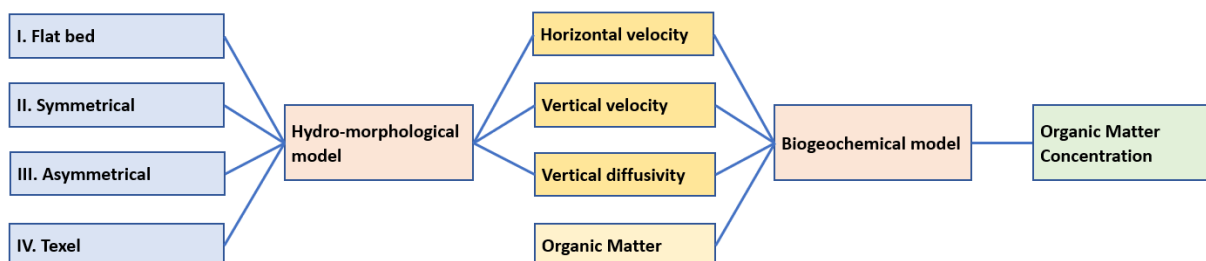


Figure 2 Flow chart of the model steps.

1.3 Research objective

The objective of this research is therefore:

To understand the distribution of organic matter over sand waves by coupling the hydro-morphological model with the biogeochemical model, and to analyse the effect of bathymetry and forcing conditions.

The research questions follow from the research objective. They are defined as follows:

1. How do the hydrodynamics fluctuate along a flat bed, a symmetrical and an asymmetrical sand wave?
2. What is the effect of the bathymetry of the sand waves and forcing conditions on the distribution of organic matter in the water column?

1.4 Method

This work is based on the hydro-morphological model of Borsje et al. (2013); Maris (2018) and van Gerwen et al. (2018) and the biogeochemical model by Soetaert et al. (2016). Figure 2 consists of a flow chart of the model steps that were taken, to couple the hydro-morphological model with the biogeochemical model, which will be shortly explained in four steps below. Further details on the method and model-steps will be described in chapter 3.

Firstly, four different cases with different model set-ups are applied, and the dimensions of each case are shown in Table 1. The first model set-up has a flat bottom with a water depth of 25 meters. This will give more insights in the hydrodynamics for the other cases. The second and third model set-up are based on van Gerwen et al. (2018), of which the initial conditions are used for the symmetrical and asymmetrical sand waves. Both have a symmetrical tide and the asymmetrical sand wave has an extra residual current in the flood tide direction, see paragraph 3.1. These two sand waves describe a sand wave in equilibrium. This has the benefit that van Gerwen et al. (2018) already explained the hydrodynamics along the sand waves. In the last model set-up, the bathymetric data from the Texel field campaign is used as input in the hydro-morphological model. However, this is not an equilibrium sand wave, which means that the hydrodynamics is not in balance with the sea bed. This will be further explained in paragraph 2.6. The Texel sand waves will give more insights on an actual sand wave field.

Next, the four cases are used as input in the hydro-morphological model. The cases differ in bathymetry and also have different forcing conditions, i.e. tidal symmetry and residual currents. For all the cases, one tidal cycle of twelve hours, with a spin-up, is run under steady conditions, i.e. no bed development. This will be further explained in the model description, see paragraph 3.1.

Thirdly, from the hydro-morphological model, the horizontal flow velocity, the vertical flow velocity and vertical diffusivity are used as input in the biogeochemical model. Together with the hydrodynamic information, the organic matter concentration is needed as input as well.

Table 1 Dimensions of the four cases.

	Description	Wave height (m)	Wave length (m)	Water depth (m)
Case I	Flat bed	0	0	25
Case II	Symmetrical sand wave	10	200	25
Case III	Asymmetrical sand wave	9	200	25
Case IV	Texel sand wave	2,6 – 3,4	170 - 220	30

Finally, in the biogeochemical model the organic matter will be produced at the water surface. Then the hydrodynamics from the hydro-morphological model are incorporated to drive the different processes in the biogeochemical model, see Figure 1. The output of the biogeochemical model is the organic matter concentration in the water column over the tidal sand waves. This will be further explained in paragraph 3.2. In this model, the same grid is used as the one from the hydro-morphological model, see paragraph 3.3.

The sand waves will also be divided in four parts, namely trough, stoss, crest and lee (Figure 1). These are points on the sand waves to understand the difference in behaviour of the hydrodynamics and the organic matter transport over a sand wave.

1.5 Outline

Chapter 2 describes the different theoretical concepts in the creation of the hydro-morphological model, using the numerical model from Delft3D, the biogeochemical model, organic matter and the field campaign near Texel. Chapter 3 describes the hydro-morphological model and the biogeochemical model with their model set-ups. Chapter 4 shows the results of the research, using the hydrodynamics used in the four different cases, the organic matter distribution over the four cases as well as some remarks for the Texel case. Finally, in the last two chapters, a discussion of the method and results will be presented and a conclusion will be given.

Theoretical concepts

2.1 Hydro-morphological model realisation

Over the years, several studies have been carried out about the behaviour of sand waves. This was first started by Hulscher (1996), who modelled the sand wave growth using linear stability analysis (LSA). After this study, several extensions have been made, for example the migration (Besio et al., 2004; Németh et al., 2002) or physical mechanisms as grain size variation (Roos et al., 2007). Some of these studies were based on LSA, but as amplitudes of sand waves increase, the non-linear effects become more important. Linear stability analyses describe the time development of arbitrary bottom configurations characterized by small amplitudes (Besio et al., 2008). Linear theory does not give any information on the actual amplitude of the features (Dodd et al., 2003).

A hydro-morphological model was created over several studies that used the numerical model Delft3D with respect to the morphological behaviour. Tonnon et al. (2007) was the first who studied an idealised sand wave by the combination of Delft3D and an artificial sand wave near Hoek van Holland. More recently, Borsje et al. (2013) reproduced the initial stage of tidal sand wave formation in Delft3D. Then, Borsje et al. (2014) implemented the influence of suspended load transport on the formation of sand waves into the model. Finally, van Gerwen et al. (2018) adopted the numerical model to study the growth of sand waves towards a stable equilibrium.

Maris (2018) used Delft3D to model the two-way coupling between sand waves and *L. conchilega*. The tubes of the *L. conchilega* were modelled as thin solid piles in Delft3D, which affects drag and turbulence. The tubes cause more bottom roughness, therefore the near-bottom flow is decreased and the turbulence is increased. Due to the decrease of near-bed velocities the sediment will be deposited between the tubes. The patches of *L. conchilega* were located where the bed shear stress was lower than the tide-averaged bed-shear stress. This suggested that patches of *L. conchilega* will settle at the troughs and lower flanks of sand waves.

2.2 Delft3D

The hydro-morphological model is made with the process-based model Delft3D. It is able to model sand waves from an initial stage to an equilibrium height and give insights into how the dynamics are influenced by physical quantities (van Gerwen et al., 2018). Compared to LSA, Delft3D can include several physical processes and the modelled sand waves in Delft3D holds for large amplitudes. Because of this, Delft3D can be used for the coupling with organic matter.

Delft3D is a numerical shallow water model, which simulates two dimensional (2DV and 2DH) and three dimensional flow (3D), sediment transport and morphology, waves, water quality and ecology and the interaction between these processes. Therefore, this model can be applied to a wide range of river, estuarine and coastal situations, because of the broad range of variables, such as wind shear, wave forces, tidal forces, etc. (Lesser et al., 2004).

2.3 Marine ecology

An ecological model predicts the behaviour of the benthic macrofauna, which are animals greater than 0.5 mm in size and live on or within the sea floor (Soetaert & Herman, 2009). These can be classified into three main feeding groups: suspension feeders, deposit feeders and/or filter feeders (Lessin et al., 2019). Some animals can even alternate between more than one feeding type, depending on the surrounding conditions or circumstances. This model aims to determine which groups of feeders will form and where they will form. This is due to the way the feeders capture their food. The main determinants for this is the velocity and/or the organic matter concentration, both from the water column and in the sediment. The biogeochemical model is a component of the ecological model.

2.4 Organic matter

The quality and concentration of organic matter that becomes incorporated in the sediment is an important characteristic of a benthic system, because of benthic fluxes and carbon mineralization (Soetaert et al., 1996). Organic matter supply is a key driver in setting the dominant functional traits of benthic communities and can have a significant impact on biogeochemical cycles in both sediments and benthic–pelagic coupling (Lessin et al., 2019) and is often extensively studied (e.g. Bianchi, 2011; van Nugteren et al., 2009). The rate of mineralization can be an indication of the amount of organic matter, which is a food source for the benthic organisms, as well as the level of biological activity occurring in the sediment. Locations with higher concentrations of organic matter could mean that the abundance of the benthic organisms is also higher, or potentially as such.

In the biogeochemical model, the organic matter comprises a mixture of suspended sources (e.g. dissolved organic matter, bacteria, marine snow and small zooplankton) that are transported largely by hydrodynamics (Soetaert et al., 2016), to reconstruct organic food supply. The organic matter in the model is expressed in terms of carbon, which is a major component of biological compounds.

2.5 Biogeochemical model

The biogeochemical model was first used in Soetaert et al. (2016), in which the interaction between tidal currents and cold-water coral mounds was investigated. This model predicted the behaviour of the organic matter that was produced at the water surface and, subjected to passive sinking, hydrodynamical transport and biological degradation (Soetaert et al., 2016). The main determinants for this was the velocity and/or the organic matter concentration, both in the water column. After the organic matter is produced at the water surface, it can be changed in several ways. The organic matter could be transported with the tidal currents, deposited by sinking with a sinking velocity and/or decay by respiration, which is incorporated through a respiration rate.

2.6 Site Texel

The fourth case of this research is the Texel sand wave, where the bathymetry of the Texel sand waves are implemented in the hydro-morphological model. The two field campaigns to a sand wave field in the Dutch North Sea were undertaken onboard the NIOZ RV-Pelagia in June and October 2017, see Figure 3 for the cross section of the sand wave (Cheng et al., submitted; Damveld et al., 2018). A Kongsberg EM302 Swath Multibeam echo sounder was used to collect the bathymetric data. These sand waves were investigated through two studies. The study of Damveld et al. (2018) showed a significantly higher epi- and endobenthos abundance in two of the sand wave troughs compared to two of the crests, indicating that sand waves affect the distribution of benthic communities. Furthermore, the study of Cheng et al. (submitted) showed a distinct sorting of sediment and a

difference in permeability along the same sand waves. As a result, this could have implications on the biota in these sand waves.

In order to compare these results with the models, the bathymetry of the Texel sand waves are also incorporated into the model so that the same sand wave dimensions are also tested with respect to the organic matter transport. The Texel sand waves are largely asymmetric, with lee slopes oriented NNE, and the studied sand waves ranging from 2.6 to 3.4 m high and 170 to 220 meter long (Cheng et al., submitted). The bathymetry of five sand waves are implemented in the hydro-morphological model. Not only does this maintain the exact dimensions from the field, but another benefit of this scenario is the result of producing five sand waves that differ in length, height and asymmetry, as opposed to the hydro-morphological model simulations that produce almost-identical sand waves. Another difference with the other three cases is the mean water depth of 30 meters instead of 25 meters. Other dimensions will be further explained in chapter 3. Finally, these sand waves are not in equilibrium, which means that the hydrodynamics is not in balance with the seabed.

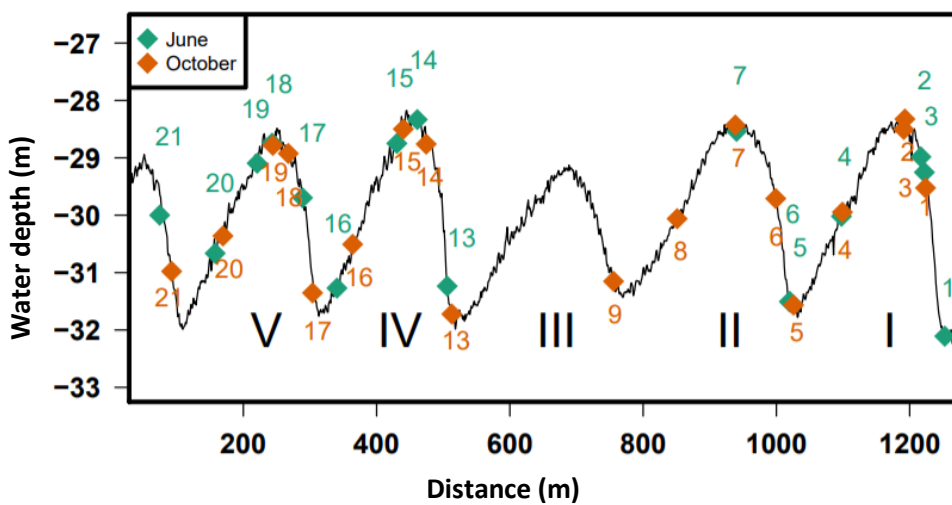


Figure 3 Cross section of the Texel sand waves (Cheng et al., submitted).

Model description

3.1 Hydro-morphological model

The hydro-morphological model is able to model sand waves from an initial perturbation to an equilibrium height and gives insight into the hydrodynamics (van Gerwen et al., 2018). However, this requires large computational efforts. Therefore, this research uses the models of van Gerwen et al. (2018), in which sand waves are already created and only some parameters have to be changed, for example wave height, wave length and water depth.

The hydro-morphological model is based on the numerical shallow water model Delft3D-FLOW (Lesser et al., 2004). The model is run in the 2DV mode, i.e. it considers flow and variation in x and z direction only, assuming that there is zero flow in y direction. It is also assumed that Coriolis effects are negligible (Hulscher, 1996). A vertical sigma (σ) layering, with 60 layers, has been applied to solve the model equations (Borsje et al., 2013). The model equations can be divided in hydrodynamic equations and transport equations. As these were described in the previous studies, only the equations of which the output will be used as input in the biogeochemical model are included here.

3.1.1 Hydrodynamic equations

In terms of the σ coordinates, the 2DV hydrostatic shallow water equations are described by the horizontal momentum equation and the continuity equation:

$$\frac{\partial u}{\partial t} + u \frac{\partial u}{\partial x} + \frac{\omega}{(H + \zeta)} * \frac{\partial u}{\partial \sigma} = -\frac{1}{\rho_w} P_u + F_u + \frac{1}{(H + \zeta)^2} \frac{\partial}{\partial \sigma} * \left(v_T \frac{\partial u}{\partial \sigma} \right) \quad (1)$$

$$\frac{\partial \omega}{\partial \sigma} = \frac{\partial \zeta}{\partial t} - \frac{\partial [(H + \zeta)u]}{\partial x} \quad (2)$$

where:

u	[m s ⁻¹]	horizontal velocity in x direction,
ω	[m s ⁻¹]	vertical velocity relative to the moving vertical σ - plane,
H	[m]	water depth,
ζ	[m]	free surface elevation,
ρ_w	[kg m ⁻³]	water density,
P_u	[N m ⁻²]	pressure gradient,
F_u	[m s ⁻²]	horizontal Reynold's stresses,
v_T	[m ² s ⁻¹]	vertical eddy viscosity.

Both horizontal and vertical velocity and the vertical diffusivity will be used as input in the biogeochemical model. The vertical diffusivity is calculated with the vertical eddy viscosity. The vertical eddy viscosity is calculated in Delft3D with the $k - \epsilon$ turbulence closure model, in which both turbulent energy k as well as the dissipation ϵ are explicitly described (Rodi, 1980), for details on the $k - \epsilon$ turbulence model formulations see Burchard et al. (2008). The vertical viscosity is estimated as:

$$v = c_\mu \frac{k^2}{\epsilon} \quad (3)$$

where:

c_μ	[-]	constant with a recommended value of 0.09 (Rodi, 1980),
k	[$m^2 s^{-2}$]	turbulent kinetic energy,
ε	[$m^2 s^{-3}$]	turbulent energy dissipation.

The vertical diffusivity is derived from the eddy viscosity (Deltares, 2014) and is estimated as:

$$D_z = \frac{v}{\sigma_c} \quad (4)$$

where:

u	[$m^2 s^{-1}$]	vertical eddy viscosity,
σ_c	[-]	Prandtl-Schmidt number, depends on the substance.

3.1.2 Sediment transport and bed evolution

The transport equations consist of the sediment transport (bedload and suspended load transport) and the bed evolution. The bedload transport uses a correction parameter for the slope effects. Because, bedload transport is affected by bed level gradients, this allows sediment to be transported downhill more easily than uphill. The suspended sediment concentration is calculated by solving the advection-diffusion equation. Finally the bed evolution is governed by the sediment continuity equation (Exner equation). The Exner equation simply states that convergence (or divergence) of the total transport rate must be accompanied by a rise (or fall) of the bed profile.

3.1.3 Model set-up

In this section the input values, following the model of van Gerwen et al. (2018) for the four cases will be described.

The input parameters of the hydrodynamic timestep, median sediment grain size, bed slope parameter and Chézy roughness are for all four cases the same as those from van Gerwen et al. (2018) and are shown in Table 2.

A tidal amplitude U_{S2} of 0.65 m s^{-1} is used in all four cases, but the asymmetrical case is extended with another hydrodynamic forcing, a U_{S0} tidal component of 0.05 m s^{-1} . This residual current causes the asymmetry of the sand wave. To create a symmetrical and asymmetrical sand wave in equilibrium, the model needs a morphological change or bed development that would cause sand wave growth and migration.

Table 2 Overview of values and units of the hydro-morphological model parameters.

Description	Symbol	Value				Unit
Chézy roughness	C	75				$m^{1/2}s^{-1}$
Bed slope correction parameter	α_{bs}	3				-
Sediment grain size	d	0.35				mm
Time step	dt	12				s
Description	Symbol	Case I	Case II	Case III	Case IV	Unit
Amp. Hor. S0 tidal velocity	U_{S0}	0	0	0.05	0	ms^{-1}
Amp. Hor. S2 tidal velocity	U_{S2}	0.65	0.65	0.65	0.65	ms^{-1}
Asymmetry parameter	A	0	0	0.26	≈ 0.35	-
Initial wave amplitude	A_0	0	0.5	0.5	-	m
Mean water depth	H_0	25	25	25	30	m

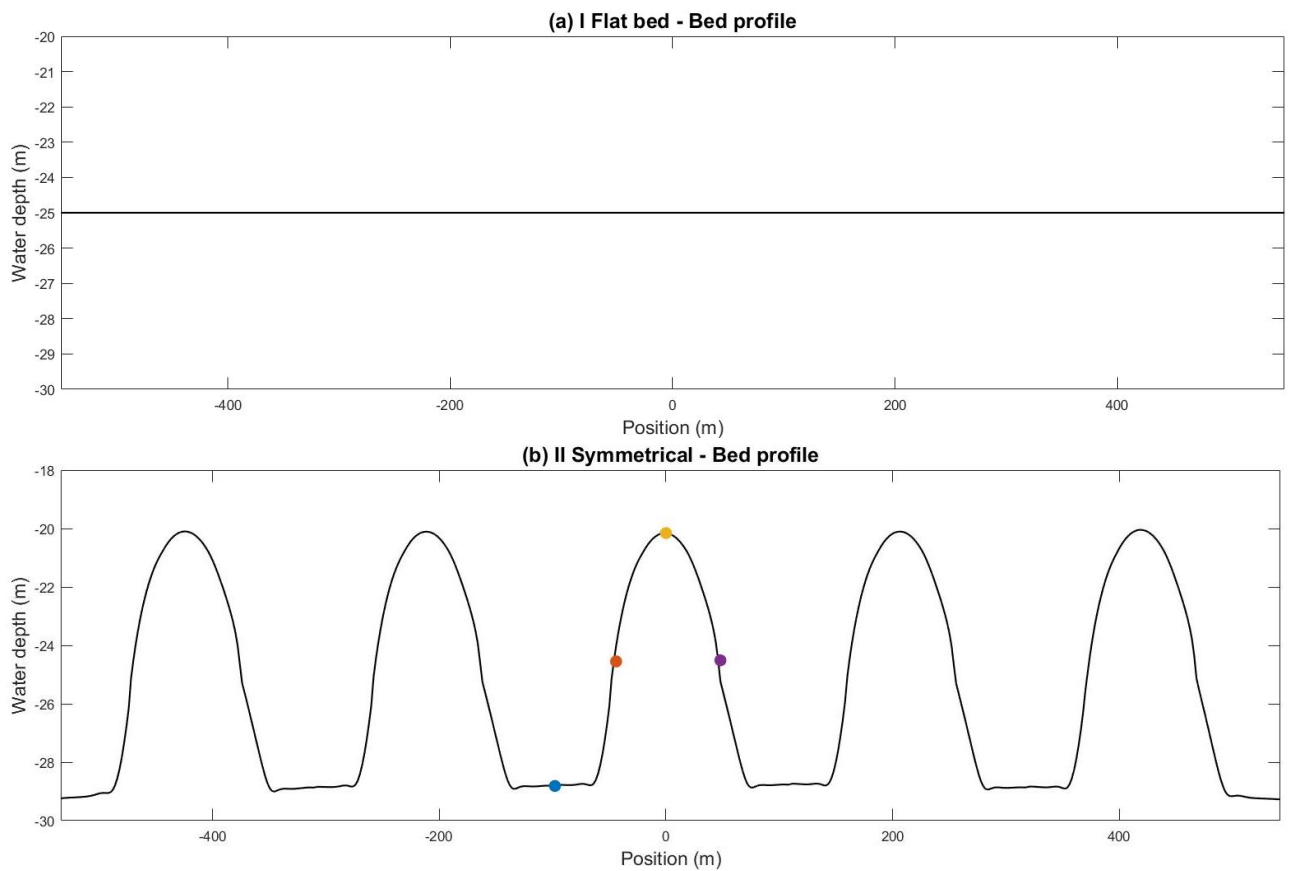
After that, both sand waves are run for one tidal cycle (S2) without morphological change. This means that the output of all four cases have no morphological change as well as a steady flow. Morphological changes occur on a much larger time-scale than the hydrodynamic changes (years vs. hours). Therefore a morphological acceleration factor (MORFAC) is introduced in the creation of the equilibrium sand waves. Here, a MORFAC of 2000 was used (van Gerwen et al., 2018). This factor is then multiplied with the bed evolution after each time step (one tidal period corresponds to 12h * 2000 = 2,7 years). Because of the morphological changes, the initial wave amplitude is set to 0.5 meter and run for 150 years. Van Gerwen et al. (2018) showed for different wave heights the development over simulation time.

The bed forms generated by the model set-ups are shown in Figure 4. However, the bathymetry of the Texel sand wave had to first be interpolated over the correct amount of grid cells, and followed by the application of a smooth function. Otherwise the hydro-morphological model would give an error.

The asymmetry is characterized as the difference between the stoss length and the lee length, divided by the sand wave length (Knaapen, 2005):

$$A = \frac{L_{Stoss} - L_{Lee}}{L_{Total}} \quad (5)$$

In this research the asymmetry parameter for case III is 0.26, with L_{Stoss} of 130 meters and L_{Lee} 76 meters. For symmetrical sand waves, $A=0$ and fully asymmetrical sand waves $A = 1$, where $L_{Total} = L_{Stoss}$ (Damen et al., 2018).



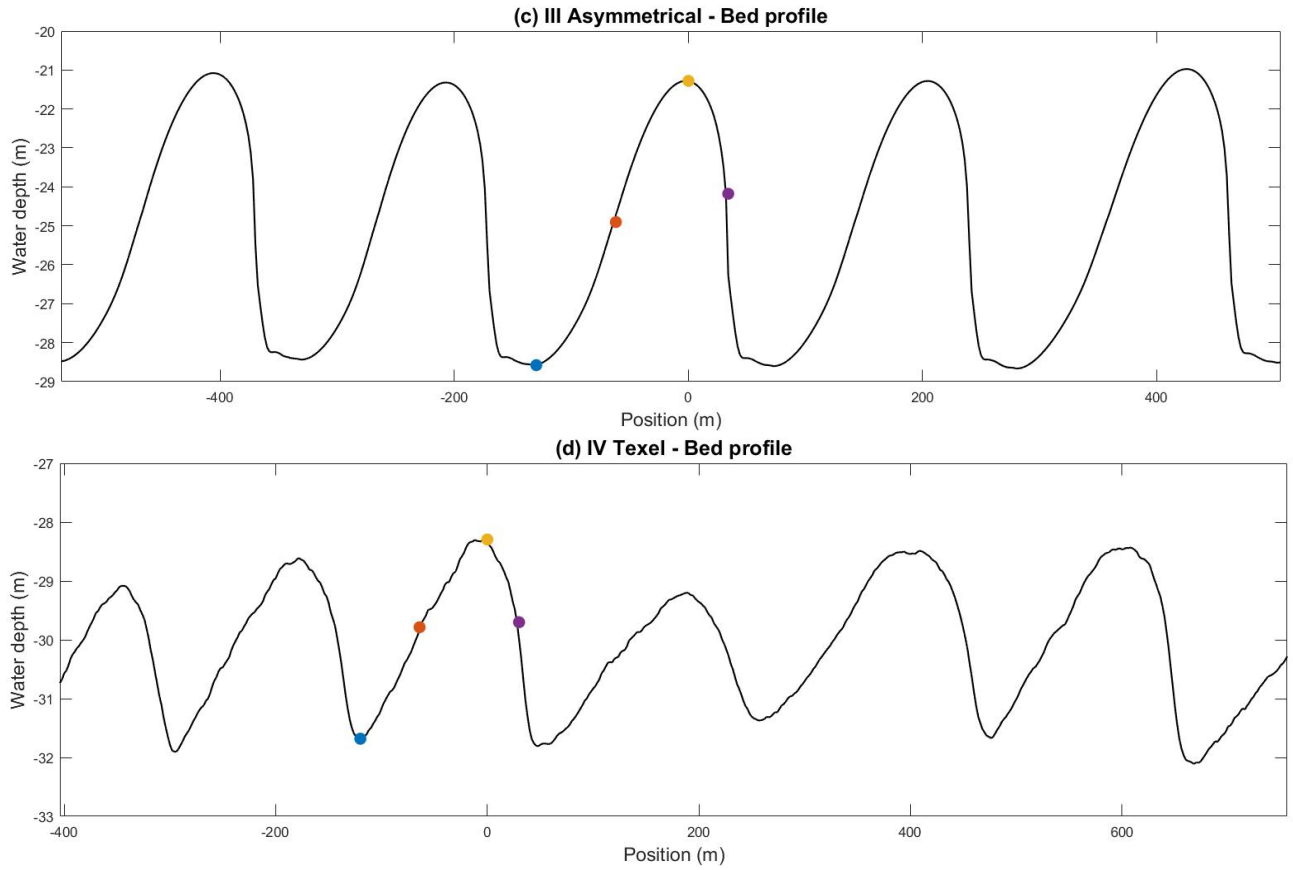


Figure 4 Bedforms of (a) case I flat bed, (b) case II symmetrical sand wave (c) case III asymmetrical sand wave and (d) case IV Texel sand wave. The four dots are the four different sand wave locations of trough, stoss, crest and lee, explained in paragraph 1.5.

3.2 Biogeochemical model

The biogeochemical model is based on Soetaert, Mohn, Rengstorf, Grehan, & van Oevelen (2016) and Soetaert & Herman (2009) and consist mainly of the following equation:

$$\underbrace{\frac{\partial C}{\partial t}}_{(1)} = \underbrace{-\frac{1}{A_x} * \frac{\partial(A_x * u * C)}{\partial x}}_{(2)} - \underbrace{\frac{1}{A_z} * \frac{\partial(A_z * v * C)}{\partial z}}_{(3)} + \underbrace{\frac{1}{A_z} * \frac{\partial}{\partial z} \left(A_z * D_z \frac{\partial C}{\partial z} \right)}_{(3)} - \underbrace{\frac{\partial}{\partial z} (w_o * C)}_{(4)} - \underbrace{k * C}_{(5)} \quad (6)$$

C	[mol m ⁻³ s ⁻¹]	organic matter concentration rate,
A	[m ²]	surface in x and z direction (Figure 5),
u, v	[m s ⁻¹]	horizontal and vertical velocity,
D _z	[m ² s ⁻¹]	vertical diffusivity,
w _o	[m s ⁻¹]	sinking rate of organic matter,
k	[s ⁻¹]	respiration rate.

The formula is a partial differential equation that expresses the rate of change in organic matter concentration, as a function of the fluxes and the biogeochemical processes: (1) Rate of change in organic matter concentration, (2) advection, (3) dispersion, (4) sinking and (5) respiration (see also Figure 1). The domain is the same as in the hydro-morphological model and the cells in the hydro-morphological model are named 'boxes' in this model. The subscript 'x' means the horizontal direction and the subscript 'z' means the vertical direction, see Figure 5. The organic matter in each box has a concentration C, units of mass per a given volume, and is located in the centre of each box.

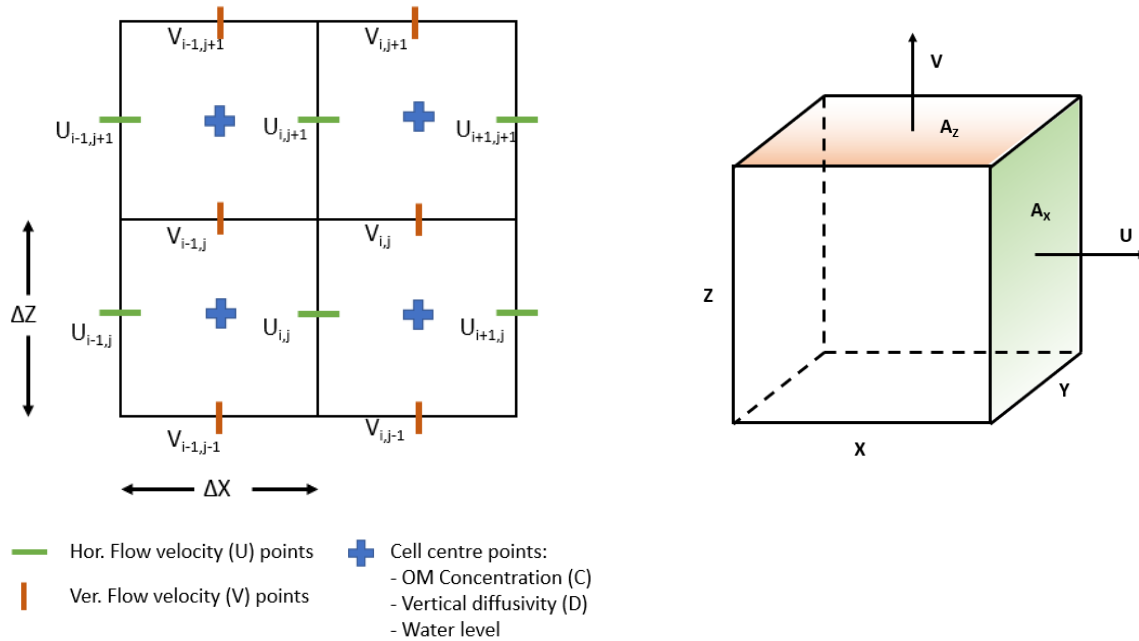


Figure 5 Numerical scheme and 3D grid for the biogeochemical model, the horizontal stripes are the horizontal velocity points, the vertical stripes are the vertical velocities points and the plus signs are the centre points.

Organic matter is produced very near the air-sea interface (e.g. from photosynthesis by phytoplankton), and sinks from the surface by gravity, while it is simultaneously being degraded (through respiration) and also transported by the currents.

The biogeochemical model is run offline from the hydro-morphological model, and uses the same grid, a staggered grid or Arakawa C-grid (Figure 5). This means that the biogeochemical model is executed in 2D as well. The model is implemented in the R-package 'deSolve' (Soetaert & Petzoldt, 2010), through the open-source software R. (R. Core Team, 2014).

3.2.1 Processes

Equation 6 shows five different processes that are used in the biogeochemical model; these were also shown in Figure 1. The first process is the rate of change of organic matter, the other four processes are described below.

Advection

The fluxes can be expressed as the product of the velocity times the concentration (Soetaert & Herman, 2009). This kind of directed movement is the advective flux, i.e., the transport of particles due to water flows as described by the second term in equation 6 and is situated in the velocity points, see Figure 5. Advection is calculated with the help of backward differencing. This means that the difference in advective flux in the box will be taken for the calculation. For instance backward differencing with horizontal advection will be:

$$\frac{\partial \text{Advection}}{\partial x} = -\frac{1}{A_x} * \frac{\left((A_{i,j} * U_{i,j}) - (A_{i-1,j} * U_{i-1,j}) \right)}{\partial x} * C_{i-0.5,j} \quad (7)$$

Dispersion

Due to random motion, organic matter has a tendency to move towards equilibrium, whenever there are differences in concentration gradients. This means the net flux will always be directed from higher to lower concentration areas. These dispersive fluxes are described as the product of a dispersion coefficient and a concentration gradient. The dispersion coefficient is the eddy diffusivity obtained

from the hydro-morphological model output, and is described by the third term in equation 6 and is situated in the centre points of the boxes. The dispersion part is calculated with the help of centre differencing. This will take the mean of the dispersion values of two cells. Because of this, the new value will be situated in the velocity points on the edges of the boxes and not in the centre, see Figure 5. For instance, a calculation of a dispersion part will be:

$$\frac{\partial Dispersion}{\partial z} = \frac{1}{A_z} * \frac{\left(A_z * \frac{D_{i-1,j-0.5} + D_{i-1,j+0.5}}{2} * (C_{i-1,j-0.5} - C_{i-1,j+0.5}) \right)}{\partial z} \quad (8)$$

Sinking

The fourth term is the sinking term, where particles sink through a water column at a certain velocity (Soetaert & Herman, 2009), such that particles in a particular box will be replaced by particles from above, while the box itself will lose particles to lower boxes. At the bottom, the organic matter leaves the water column to settle on the sediment surface. This is described by the sinking rate times the organic matter concentration in the water column.

Respiration

Finally, there is the respiration, the process that supplies an organism with the energy required for growth and maintenance and that causes the organic carbon concentration to decline through consumption by organisms. Here it is assumed that organic matter decay proceeds at a first-order rate, so the respiration in general is a respiration rate times the concentration.

3.2.2 Model set-up

This section describes the model set-up of the biogeochemical model.

Boundary conditions

The biogeochemical model has three boundary conditions:

1. At $z = 0$; at the water surface is a flux boundary which represents the growth of the organic matter:

$$w_o * C_{z=0} = F \quad (9)$$

2. At $z = z_b$; at the sea bed is a zero gradient boundary, which leads to deposited organic matter by sinking:

$$\frac{\partial C}{\partial z(z=z_b)} = 0 \quad (10)$$

3. At both x boundaries, these are also zero gradient boundaries, holds:

$$\frac{\partial C}{\partial x(x=x_b \text{ or } x=x_a)} = 0 \quad (11)$$

During flood tide the flows have positive values, and the model is calculated in the positive x-directions. During ebb tide it is the opposite, and the flows have negative values and the model is calculated in the negative x-direction. In the biogeochemical model, there are two possibilities for processes in the x-direction. When the model is repeated, then the model is cycled such that the lateral cell will be used as the first cell in the domain. When there is no cycle, the grid cells of the first column upstream will be used and the transport will be zero at the first column.

Initial conditions

To initialise the organic matter in the water column, the steady-state solution of equation 6 is implemented. The concentration does not change over time and the flow velocities are zero, which result in the following equation:

$$\frac{\partial C}{\partial t} = 0 = -\frac{\partial}{\partial z}(w_o * C) - k * C \quad (12)$$

With boundary condition one at $z = 0$: $w_o * C_{z=0} = F$, the analytical solution is:

$$C(z) = \frac{F}{w_o} * e^{\left(\frac{-k}{w_o} * z\right)} \quad (13)$$

Mass balance

The dynamic simulation imposes the advective flows and the diffusion coefficients obtained from the hydro-morphological model. To prevent numerical creation or destruction of mass, the mass balance of each box has to equal zero. Unfortunately, this was not the case with the provided velocities from the hydro-morphological model, probably because the velocities have been re-gridded; the horizontal velocity data are averaged to water level points, i.e. in the centre of the boxes (Figure 5) .

This was solved by assuming that all the vertical velocities provided from the hydro-morphological model were correct. Based on the horizontal velocities of each box of the first column upstream and the given vertical velocities of all boxes, the mass balance equation was used to estimate the other downstream horizontal velocities. After that, both the horizontal flow velocities from the estimation with the mass balance equation (estimated) and the given horizontal flow velocities from the hydro-morphological model (modelled) of all boxes of each time step were compared, and this showed a small but acceptable difference (Figure 6).

Input

At the surface, a constant flux of $1.2 * 10^{-6} \text{ mol m}^{-3} \text{ s}^{-1}$ was imposed. The sinking rate of $5.9 * 10^{-5} \text{ m s}^{-1}$ and the first order decay rate or respiration rate of $5.8 * 10^{-7} \text{ s}^{-1}$ are representative for the decay of freshly produced organic matter, see Table 3.

Table 3 Overview of values and units of the biogeochemical model parameters.

Description	Symbol	Unit	Value
Organic matter rate, surface source	F	$\text{mol m}^{-3} \text{ s}^{-1}$	$1.2 * 10^{-6}$
Respiration rate	k	s^{-1}	$5.8 * 10^{-7}$
Sinking rate	w	m s^{-1}	$5.9 * 10^{-5}$

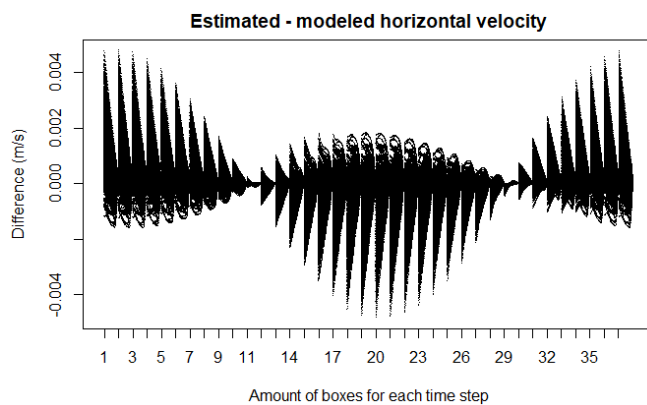


Figure 6 The difference between the estimated and modelled horizontal velocity of an asymmetrical sand wave.

3.2.3 Assumptions

Generally, the biogeochemical model in this study used the following assumptions:

- Based on equation 6 and the work of Soetaert et al. (2016), the horizontal transport ignores mixing while the vertical transport included vertical mixing. Each box had a horizontal and vertical velocity, vertical diffusivity, organic matter concentration, a respiration term and a vertical sinking term.
- The vertical flow velocities from the hydro-morphological model were assumed to be correct, see mass balance.
- The seabed and both x-boundaries are zero gradient boundaries, which means that the change in organic matter was assumed to be zero at these boundaries.

3.3 Grid

The calculation grid in the hydro-morphological model was a sigma grid. The grid has a variable resolution in both the x- and z-directions (Figure 5 and Figure 7). The distance between the horizontal grids along the sand waves ('x') was two meter. Towards the lateral boundaries, the distance of the grids increase and the resolution decreases. The vertical resolution consisted of 60 layers, with a decrease in actual height of the layers from the water surface towards seabed ('z'), see Figure 7. The flow velocities, advection and dispersion were positioned as shown in Figure 5, which means that the surfaces were different as well. The distance between the cells in the y-direction was set to two meters for the calculation of the surfaces. All of this is sufficient to accurately describe the flow field (van Gerwen et al., 2018). The centre of the domain is based on a sinusoidal wave (Figure 4), and the outer waves were caused by an envelope function, to ensure a gradual transition from the flat bed towards the sand wave field.

The grid for the asymmetrical sand wave, case III, is almost the same. The two meter grid resolution was extended into the direction of the migration. This means the asymmetrical case has more grid cells or boxes in the x-direction. The asymmetrical sand wave had 1808 grid cells while the other cases only contained 808 grid cells.

Riemann boundary conditions were imposed at the lateral boundaries. The tidal flow will cross the open boundary without being reflected back into the computational domain.

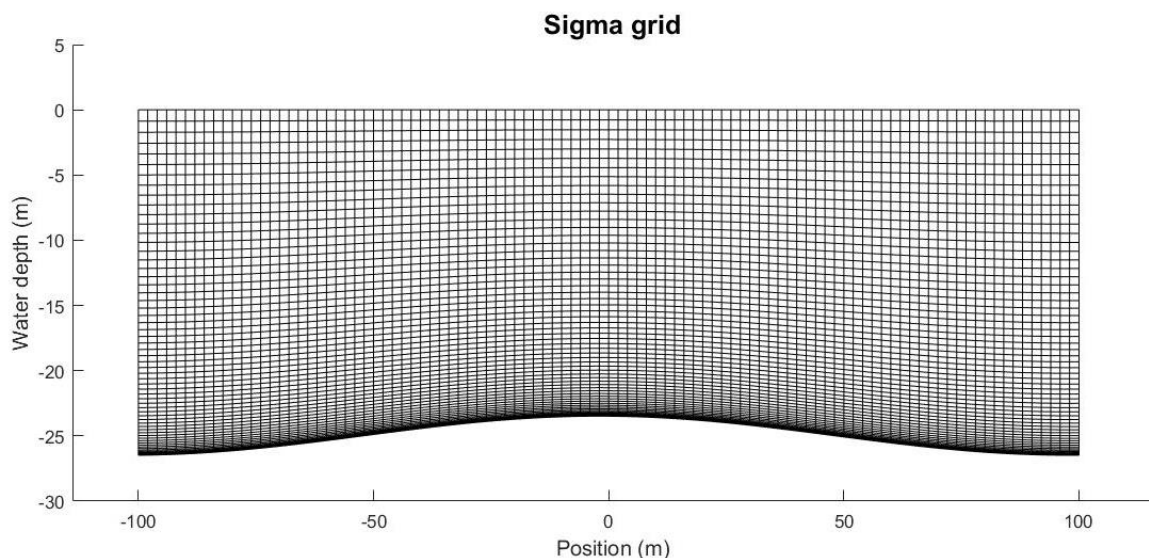


Figure 7 Sigma grid of one symmetrical sand wave.

Results

This chapter describes the results of the coupling between the hydro-morphological model and the biogeochemical model. The first paragraph will describe the general results, and also the important considerations for the other results. The second paragraph will dive into the hydrodynamics along the sand waves and the output of the hydro-morphological model will be described. The hydrodynamics will give more insights in the results of the organic matter concentration and transport, which will be described in the third paragraph. Paragraph four will show some remarkable results in the Texel case. Finally, the last paragraph will combine the hydrodynamic results with the organic matter results, to give a physical explanation of the transport of organic matter over the sand waves.

4.1 General

The hydro-morphological model was run over four different cases, with each one using the same tidal cycle as input. Thus, the timing of the flood, ebb and slack tide are identical in each case, see Figure 8. However, the flow velocity values were different for each case, because of the difference in bathymetry. At the beginning, the flow starts as flood tide, and the flow direction is in the positive x-directions (from left to right) and has positive values. At approximately half way through the tidal cycle, the flow becomes ebb tide, and the flow direction reverses in the negative x-direction (from right to left) and has negative values.

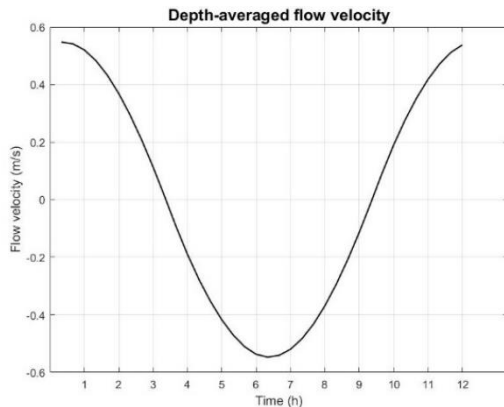


Figure 8 Depth-averaged flow velocity, positive values mean flood tide and negative values mean ebb tide.

4.2 Hydrodynamics

4.2.1 Flow velocity

To understand the movement of the organic matter along the sand waves, the hydrodynamics have to be well understood. The output of the hydro-morphological model in Delft3D was used as input in the biogeochemical model. This means that the transport of organic matter can be explained by the hydrodynamics. The tide-averaged flow velocity will give more insight in the flow velocities, by showing the net flow velocity of one tidal cycle (Figure 9). The colours in the figures make the directions of the flow more visible. Blue indicates movement to the left and red indicates movement to the right. The tide-averaged velocity for the flat bed (case I) is zero everywhere, and the flow in both directions have the same values. For the symmetrical sand wave (case II), the circulation cells are clearly visible (Figure

9a). Because of the symmetrical tide and the symmetry in the sand wave, these circulation cells occur. This is significant because the tide-averaged circulation explains the sand wave growth, as shown by Hulscher (1996). The tidal flow moving upslope is larger than the flow moving downslope. Furthermore, the opposite effect by gravity, which cause a downward movement of the grains, is also smaller than the upward flow movement. Thus, the residual circulation induces a net sediment flux towards the crest of the sand waves. In contrast, case III and IV are both asymmetrical sand waves. In case III a residual current is present which caused a disturbance of the circulation cells such that the convergence of sediment no longer occurs exactly at the crest (van Gerwen et al., 2018). Figure 9b shows the tide-averaged flow velocity of case III. Case IV also displays the same results, but the sand wave height is much smaller and as a consequence, the blue zone as well. During the ebb phase, the tidal amplitude is lower than during the flood phase. Therefore, the tide-averaged flow velocity is in the same direction as the residual current. This residual flow will cause a net migration in the same direction and facilitate the development of asymmetry in the sand waves.

Generally speaking, for the asymmetrical cases, the flow will overshoot the crest and cause a circulation on the lee side of the sand wave. This generates an upward velocity from the trough directed to the crest, which produces a kind of weak point on the lee side. And as a consequence of the upward velocity, vectors above the crest are also pointed upwards. Furthermore, the flow velocities are lower on the lee side and in the trough compared with the other positions along the sand wave. Whereas the tide-averaged flow velocity is higher in the water column for asymmetrical sand waves, it is actually higher near the sea bed for the symmetrical sand waves. This can be explained by the near-bed velocity over time.

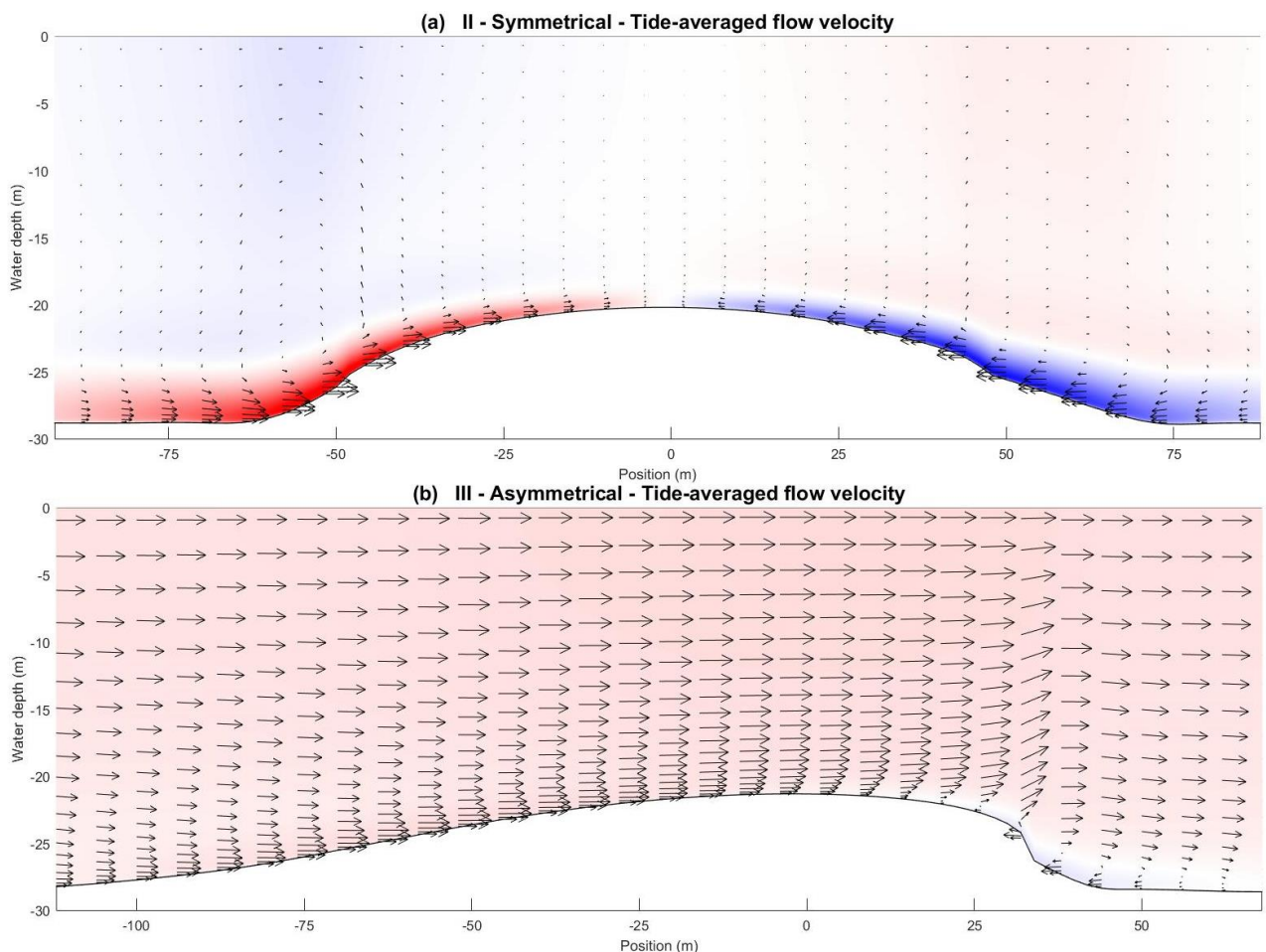


Figure 9 Tide-averaged flow velocity for (a) symmetrical and (b) asymmetrical sand wave, based on van Gerwen et al. (2018).

4.2.2 Near-bed velocity

The near-bed velocities show almost the same results in all four cases, see Figure 10. For each case, the average near-bed velocities in order to the five lowest layers for the four different locations on the sand wave are shown (the four locations are shown in Figure 4). The trough shows the highest velocities for the flat bed case, because the flat bed has a constant water depth of 25 meter while the troughs in all other cases are located at greater water depths. Thus, the opposite is also true for the velocities on the crest, which means that the near-bed velocities are lowest here for the flat bed case. As everything in regards to flow is related to the water depth, a smaller water depth will result in faster velocities under the same flow conditions.

During flood tide, the near-bed velocity shows higher values on the stoss side than on the lee side. During ebb tide, the reverse is true and the near-bed velocity is higher on the lee side than on the stoss side. Generally, during flood the flow will accelerate from trough through the stoss to the crest and overshoot the latter, which results in lower velocities on the lee side. Although this was already explained in the previous paragraph, it is worth nothing that the near-bed velocity also holds true when the flow is reversed, such as during ebb tide on the stoss side.

Overall, the near-bed velocity hardly shows any difference between the symmetrical and asymmetrical cases. On the crest, during ebb tide, the flow velocity is higher for the symmetrical sand wave. Furthermore, the asymmetrical and Texel sand wave shows a bend in the lines near slack tide, because of the asymmetry. In order to further clarify the difference between the stoss and lee side for the symmetrical and asymmetrical sand wave, the vertical flow velocity also needs to be considered.

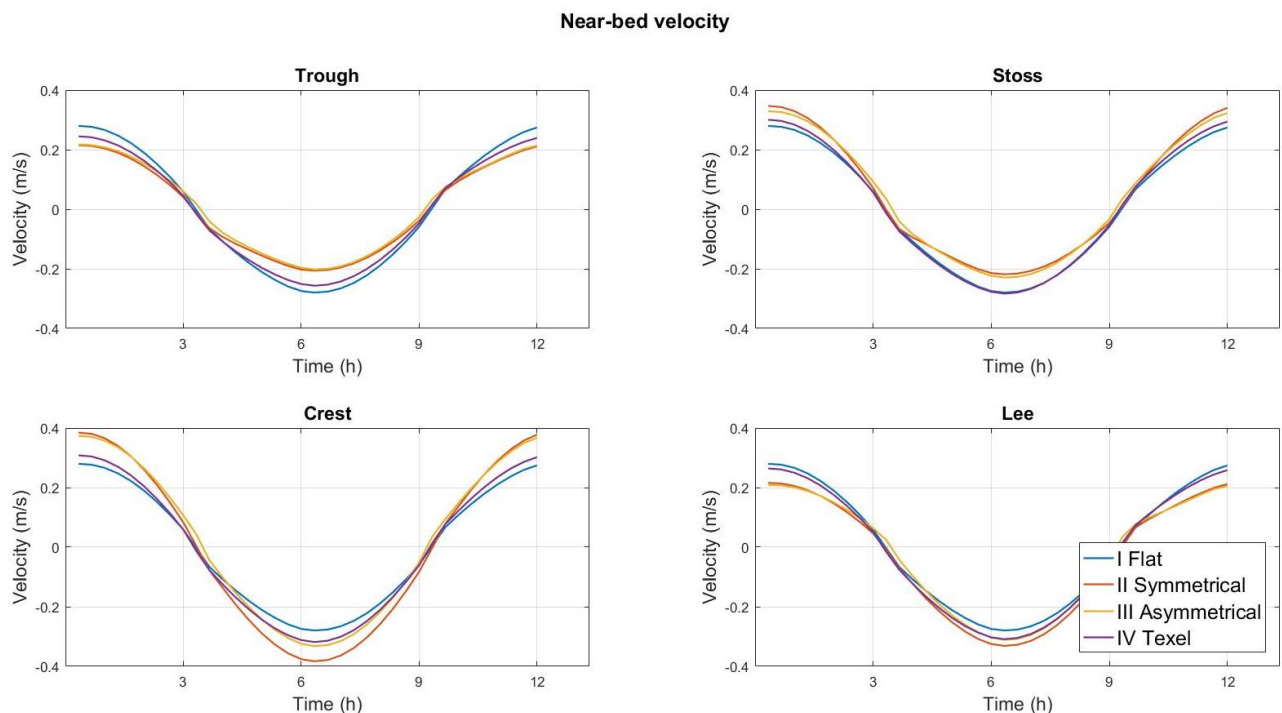


Figure 10 The average near-bed velocity in order to the five lowest layers of the four cases at four different places.

4.2.3 Vertical velocity

From the tide-averaged velocity (Figure 9b) an upward flow movement downstream of the crest was demonstrated for the asymmetrical case. This is because of the circulation on the lee side of the sand wave, which pushes the flow upwards, over the crests. The symmetrical case shows much of this vertical movement, because of the tide-averaged circulation forming on both sides of the sand wave.

Figure 11 shows a comparison of the vertical velocities for the symmetrical and asymmetrical case during ebb and flood tide for the stoss and lee sides. The vertical velocities are the highest during ebb and flood tide, and the lowest during slack tide.

At flood the flow is moving downwards on the stoss side and upwards on the lee side, for both symmetrical and asymmetrical cases (positive values are upward and negative values are downward). This is largely the result of a decrease or increase in water depth. The vertical velocities for the asymmetrical sand wave are higher on the lee side and lower on the stoss side, compared to the symmetrical sand wave. During ebb tide the vertical velocities for symmetrical and asymmetrical sand wave differ only on the stoss side, while for the asymmetrical sand waves the velocities are lower.

Lastly, the vertical velocities for the symmetrical case show nearly the same values for stoss and lee, during both flood and ebb tide. But the same does not apply for the asymmetrical sand wave, where the vertical velocities on the lee side during flood are much higher compared with the other areas of the sand wave, and the stoss side shows very low values. Because of the asymmetry in both sand wave shape and tidal flow, the vertical velocities are much higher on the lee side. The vertical velocities show circulations along the sand waves, and these circulation cells produce a higher vertical diffusivity, which will be further explained in the next paragraph.

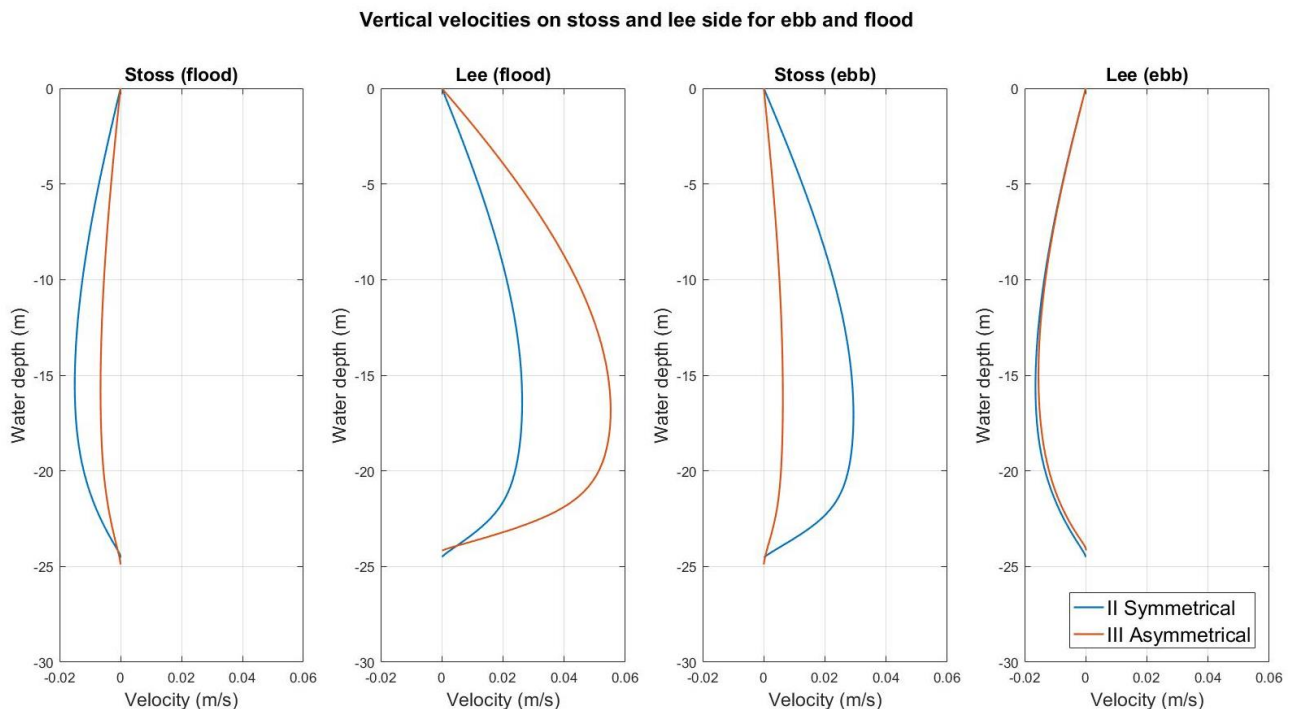


Figure 11 Vertical velocities for symmetrical and asymmetrical case on stoss and lee side for ebb and flood.

4.2.4 Diffusivity

The vertical diffusivity is a vertical turbulent transport of fluid or a turbulent mixing due to flow processes (Soetaert et al., 2016). The higher the diffusivity of water, the faster they will mix into each other. As such, lower diffusivities would be expected at the lowest flow velocities. Indeed, both horizontal and vertical flow velocities are almost zero during slack tide. However, Figure 12 shows a delayed response in the depth-averaged diffusivity values, where the smallest velocities are found during slack tide, but the smallest diffusivities occur a short while after that. Perhaps, the diffusivities respond to the flow velocities. Conversely, the highest diffusivities are found when both vertical and horizontal velocities are the highest.

For this study, the pattern of the diffusivities are the same for all cases. However, there is one clear difference between the cases, namely the Texel case, where the vertical diffusivities are higher during flood and ebb tide because it has the largest water depth of all. In the other three, there are hardly any differences in diffusivity. On the stoss and lee side, the vertical diffusivity seems to be the same as the vertical velocities, with higher diffusivity on the stoss side during flood and higher diffusivity on the lee side during ebb. Comparing all cases with the flat bed case (blue line), it makes the change of the diffusivities more visible, and this means that the bathymetry does change the vertical diffusivity. Furthermore, there is a small difference between the symmetrical and asymmetrical cases (II and III), where the latter case there has higher diffusivity at all four positions on the sand wave during flood.

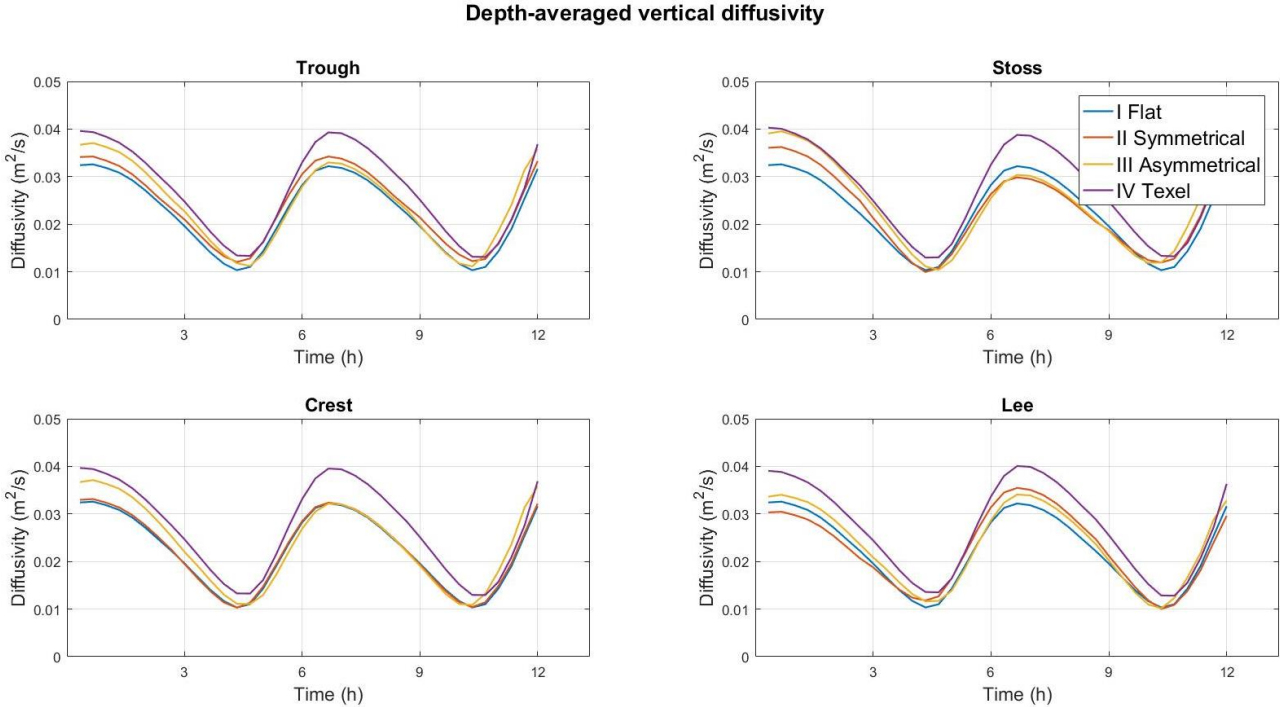


Figure 12 Vertical diffusivity for all cases at the four locations on the sand wave.

4.2.5 Slack tide

During slack tide, the flow direction begins to reverse. At approximately three hours into the model run, the flow switches from flood to ebb tide and at approximately nine hours another reversal occurs. During slack tide, the model results show a quicker change near the seabed than at the water surface. Figure 13 shows the change from ebb to flood tide for trough, stoss, crest and lee. All four locations show a different flow direction or a higher flow velocity near the seabed, compared to the water surface. However, this difference is not likely a consequence of the bathymetry (cases II – IV), because the flat bed also shows the same results.

Although, there is minimal variability between the positions on the sand waves, one such difference is that changes from ebb to flood tide happens more quickly at the trough compared to the crest (Figure 13). As such, the flow reversal happens sooner in the former than in the latter. Furthermore, the asymmetrical sand wave (case III, yellow line) is significantly shifted as compared to the other three lines. But nevertheless, the shape of the line is still the same, and demonstrates larger velocities near the seabed compared to the water surface.

Horizontal flow velocity during slack tide (t = 9,3h)

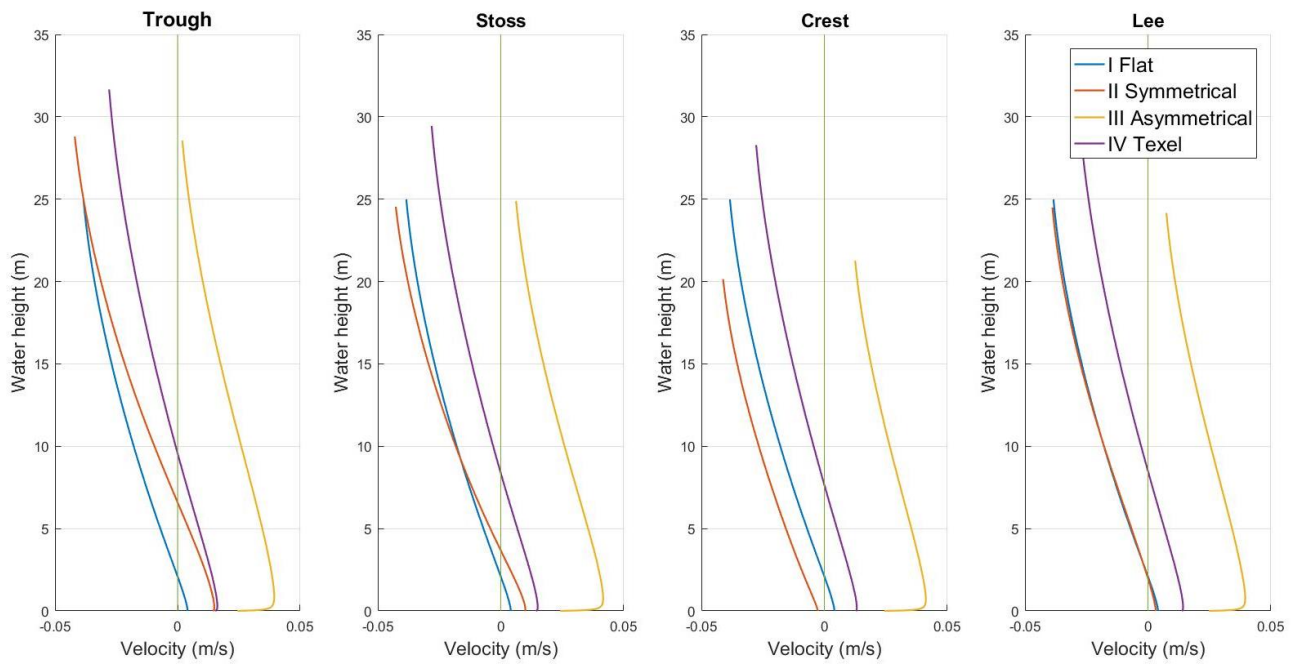


Figure 13 Horizontal flow velocity for all the cases at the four sand wave positions during the change from ebb to flood tide.

4.3 Organic matter

From the coupling of the two models, the results show a difference in organic matter distribution along the sand waves. During a tidal cycle of twelve hours, four features are observed:

1. During flood the organic matter shows an increase in concentration on the lee side, just above the trough.
2. At approximately $t = 3.0$ hours, the flow is undergoing slack tide and the organic matter is transported in the negative x-direction.
3. Subsequently, the flow becomes ebb tide at approximately $t = 6.0$ hours and the organic matter concentration starts increasing on the stoss side.
4. Finally, at approximately $t = 9.0$ hours, the flow again reverts to slack tide and the organic matter will be transported in the positive x-direction.

For the flat bed case, no difference can be observed and the concentration varies between 0.0042 and $0.0043 \text{ mol m}^{-3}$. The highest concentrations are found on the water surface. On the other hand, the organic matter concentration of the other three cases vary between 0.0020 and $0.0120 \text{ mol m}^{-3}$. For these, the bathymetry very clearly has an influence on the organic matter concentration.

Below the increase of the organic matter concentration will be further explained in the first paragraph, and the transport of organic matter in the second paragraph. The third paragraph describes the interaction of organic matter, horizontal and vertical flow velocity and vertical diffusivity on the lee side of the asymmetrical sand wave (case III).

4.3.1 Tide-averaged

Cases II - IV show a difference in the distribution of organic matter. Figure 14 shows the tide-averaged organic matter concentration for the symmetrical and asymmetrical cases, which presents distribution of the organic matter over one tidal cycle. The Texel case shows the same results as the asymmetrical case. In the symmetrical case, both the tide and sand waves are symmetrical. Consequently, the highest concentrations are found at both the lee and stoss side, depending on the tidal phase. However, Figure 14a shows a slight difference, as the sand wave (case II) is not completely symmetrical (this depends on the output from the hydro-morphological model). But due to the asymmetrical sand wave (case III), there is a residual current and an asymmetry sand wave shape, thus the highest organic matter concentrations are only found on the lee side.

4.3.2 Organic matter over time

In Figure 15, the increase and decrease of organic matter concentration is shown over one tidal cycle, for the asymmetrical sand wave (case III) at the stoss, crest and lee sides. After three hours the organic matter concentration increase on the stoss side and decrease on the lee side. After nine hours the organic matter concentration decrease on the stoss side and increase on the lee side. But the difference in concentration is much higher on the lee side due to the asymmetry.

The transport of the organic matter can be observed as well, where the lee side shows a small decrease in concentration at the start and a large decrease nearly after three hours. The decrease in concentration is indicative of organic matter transport. Following the slack tide, the concentration remains constant and organic matter concentration will increase on the stoss side. Then, following slack tide at nine hours the organic matter concentration increase on the lee side. At approximately three and nine hours, the flow conditions are at slack tide and nearly zero. The transport is visible on the crest as well, where there are three peaks just after three and after nine hours. The peaks show

that the organic matter will be transported at least over three sand waves (three peaks). The increase in organic matter concentration occurs on every sand wave, and the organic matter is moved first to the next sand wave and then the one after that. The peaks show also an decrease, because of diffusion.

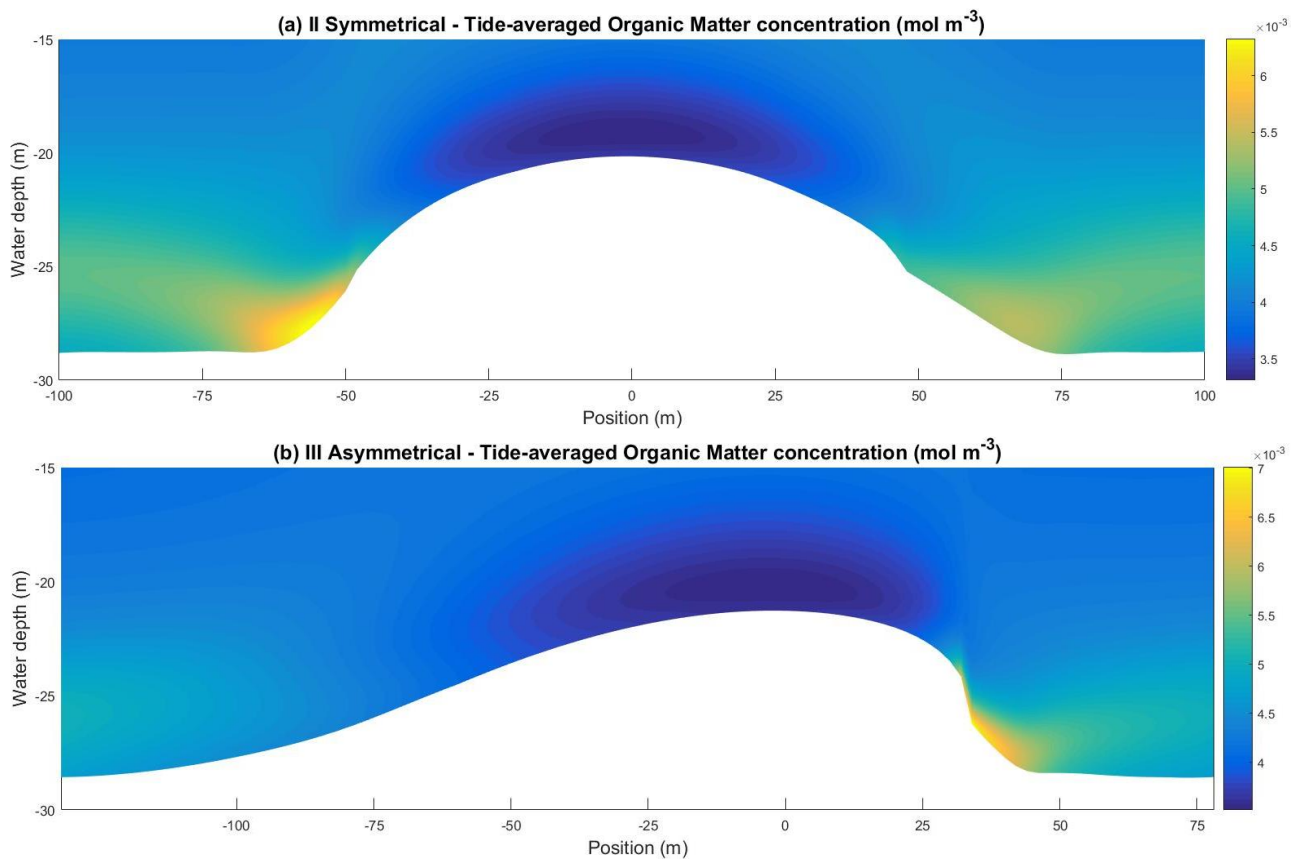


Figure 14 Tide-averaged organic matter concentration for the (a) symmetrical and (b) asymmetrical case.

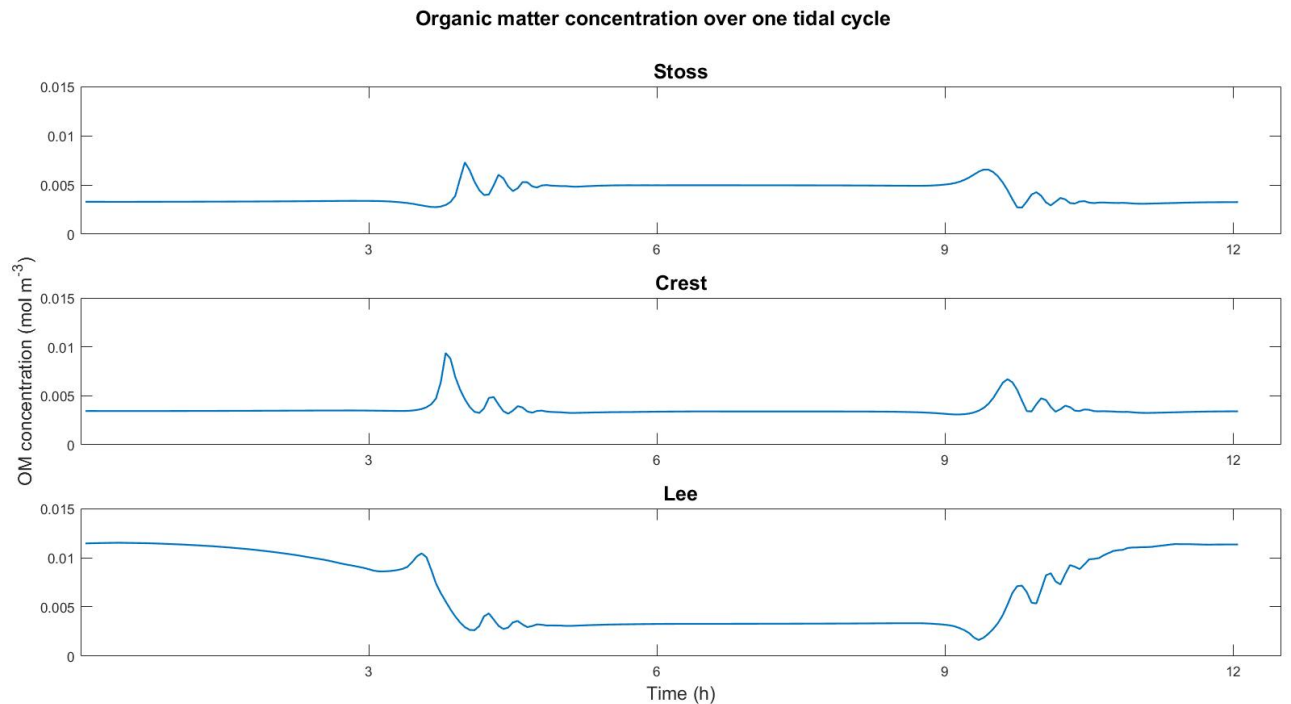


Figure 15 Organic matter concentration over one tidal cycle for the crest, stoss and lee side on the asymmetrical sand wave. The peaks at $T=3$ and $T=9$ indicate the transport of organic matter. The first peak is the organic matter concentration of the first sand wave, the second peak of the second sand wave and so on. The three peaks show a decrease because of diffusion.

4.3.3 Lee side of the asymmetrical sand wave

The tide-averaged organic matter concentration show higher concentration on the lee side of the asymmetrical sand wave. Figure 16 shows the relationship between the organic matter with the horizontal and vertical flow velocity and the vertical diffusivity. All are the mean in order to the five lowest cells at one position on the lee side of the asymmetrical sand wave.

Figure 16a displays the vertical flow velocity on the left side and the organic matter concentration on the right side. After flood tide, both the organic matter concentration and the vertical velocity shows a decrease. During slack tide the organic matter concentration quickly decreases and the vertical flow velocity is almost zero. Subsequently, both vertical flow velocity and the organic matter is constant over time during ebb tide. Finally, both show an increase as the tide switches back to flood again. Since there is almost an identical pattern with both vertical flow velocity and organic matter concentration, there could potentially be a direct link between them.

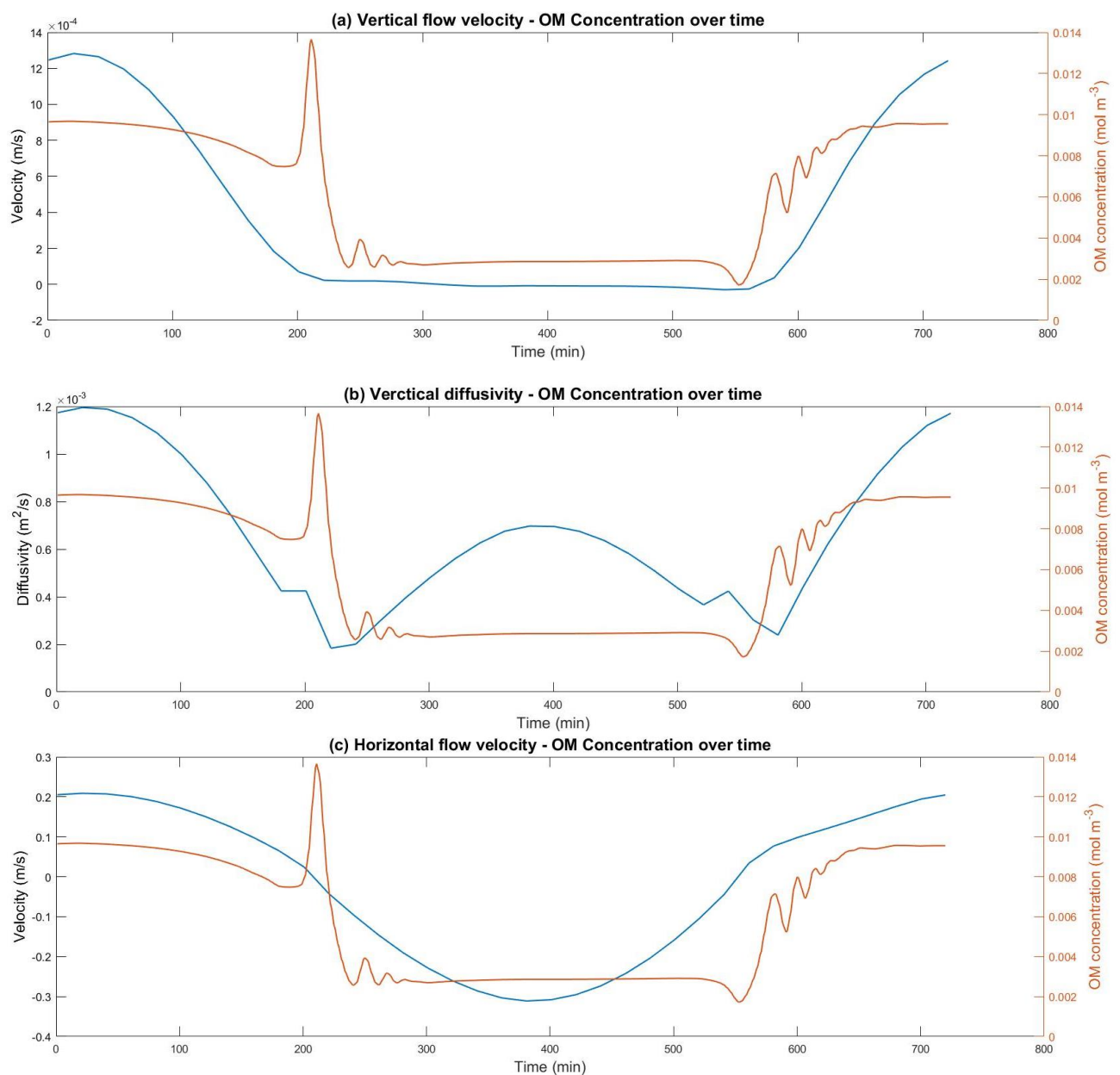


Figure 16 (a) Vertical flow velocity, (b) vertical diffusivity and (c) horizontal flow velocity with organic matter concentration at one position on the lee side of the asymmetrical sand wave (case III) over one tidal cycle.

One remark is the location on the lee side, the bathymetry has an influence on the vertical flow velocity. When the slope of the lee side is steeper, the vertical flow velocity will be higher for example.

Figure 16b also shows the vertical diffusivity on the left and the organic matter concentration on the right. Both the decrease after flood tide and increase before flood tide is observed. During ebb tide the diffusivity similarly show an increase, although less than during flood tide. The decrease and increase of both could also potentially be a direct link between the organic matter concentration and the vertical diffusivity.

Figure 16c displays the horizontal flow velocity on the left side and the organic matter concentration on the right side. When the horizontal flow velocity becomes ebb tide. the organic matter concentration shows a decrease and when the horizontal flow velocity becomes flood tide, the organic matter shows an increase in concentration. During ebb tide the organic matter concentration is constant.

4.4 Texel

Thus far, the hydrodynamic results and organic matter distribution have been shown for the first three cases. In the Texel case (IV), the sand waves are also asymmetrical in shape and thus also have the same results and observations as the asymmetrical sand waves from case III. However, because of the difference in asymmetry of the five sand waves there are a few notable observational differences, which will be described below.

4.4.1 Tide-averaged

The tide-averaged organic matter concentration shows the highest concentrations above the trough on the lee side, see Figure 17. Comparing the Texel sand waves, sand wave one has the highest concentration and sand wave three has the lowest concentration, due to the small difference in dimensions between the sand waves. The dimensions of the sand waves, the organic matter concentrations and the asymmetry parameters (equation 5) are presented in Table 4. Sand wave three has a smaller wave height and larger wave length compared with the other four. For the organic matter concentration, the maximum concentration of the tide-averaged values between crest and trough on the lee side is taken.

Table 4 Overview of values for the Texel sand waves.

	Wave height (m)	L (m)	L_{Stoss} (m)	L_{Lee} (m)	Asymmetry parameter	OM Concentration
I	3.65	192	132	60	0.306	0.0048
II	3.19	218	150	68	0.376	0.0047
III	2.17	210	140	70	0.333	0.0045
IV	3.51	170	120	50	0.412	0.0047
V	3.07	172	116	56	0.349	0.0046

4.4.2 Wave height

Figure 17 shows a difference in organic matter concentration for the different Texel sand waves. There appears to be a relationship between the dimensions of the sand waves and the organic matter concentration. A higher asymmetry parameter would signify a higher instantaneous circulation process and lower velocities on the lee side. However, the comparison of organic matter concentration with the asymmetry parameter showed no relations. Figure 18 displays the relationships between wave height of the five sand waves and the organic matter concentrations. These five dots show almost a linear increase in concentration and wave height, except for sand wave IV. Table 4 shows a larger asymmetry parameter and a higher wave height for sand wave IV compared to sand wave II, but nevertheless with the same concentration. This could mean that the asymmetry of the sand wave does affect the amount of organic matter. However, the conclusions would be more robust where more than just five sand waves are being compared and the concentration differences are nihil.

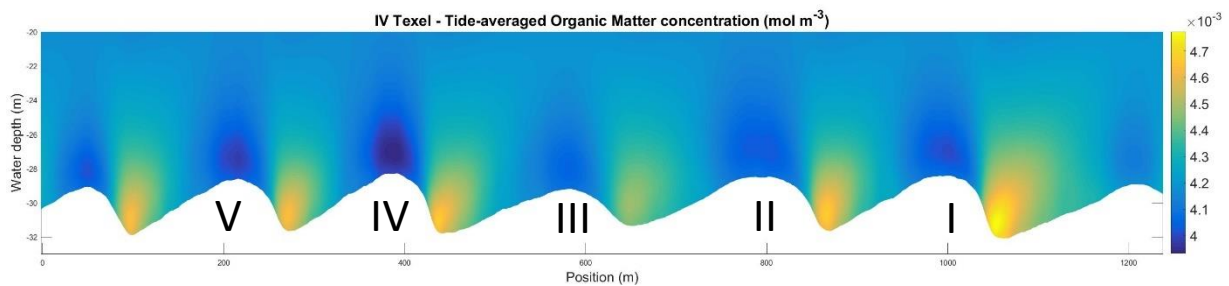


Figure 17 Tide-averaged organic matter concentration for the Texel case (IV).

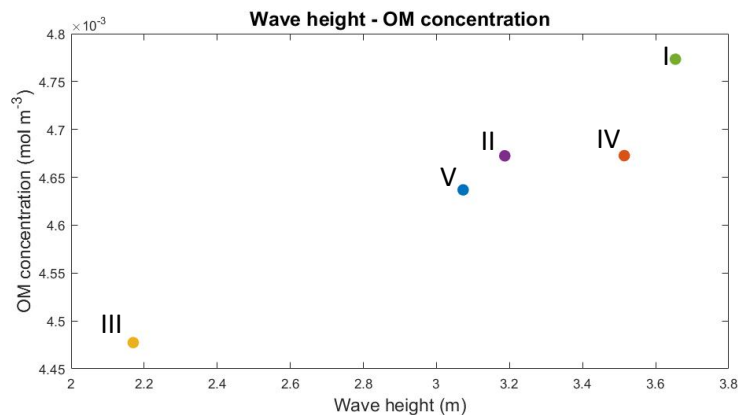


Figure 18 The organic matter concentration versus the different wave heights of the Texel sand waves.

4.5 Physical explanation

As found in the model simulations, two behaviours are visible: increase in organic matter concentration during flood and ebb and the transport of organic matter concentration in the water column during slack tide. This section describe the physical explanation for these two behaviours in which the hydrodynamics (paragraph 4.2) and the organic matter (paragraph 4.3) will be combined.

The tide-averaged flow velocity in the asymmetrical case shows a tide-averaged circulation process on the lee side of the sand wave. This will be the case as well during flood and ebb tide, but as an instantaneous circulation. This will clarify the increase in concentration of the organic matter. This process during flood as an example is showed in Figure 19. The near-bed flow velocities show higher velocities on the stoss side during flood and higher velocities on the lee side during ebb. This is because of the decrease in water depth, which results in an acceleration (1) of the flow on the stoss side. Because of this the flow will overshoot (2) the crest, which result in lower velocities on the lee side.

After the sand wave the water depth increase and the flow will decrease and will pointed downwards. This cause an instantaneous circulation (3) on the lee side of the sand wave. The ensuring instantaneous circulation, flow is then directed to the crest. Furthermore, the vertical flow velocities show an upward movement during flood tide on the lee side. This process causes weak point (4) on the lee side, where the organic matter shows an increase in concentration.

This also explains why the organic matter concentration has an lower increase on the stoss side of the asymmetrical sand wave. Because the steepness of the stoss side is lower compare to the lee side and both sides of the symmetrical sand wave. Here, the overshooting process and the instantaneous circulation is lower or even not existing.

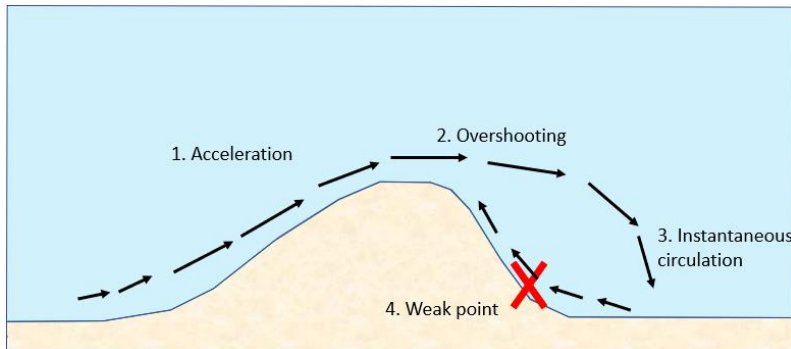


Figure 19 Process that causes an increase in organic matter concentration during flood tide.

The second behaviour is the transport of the organic matter during slack tide. The process behind this is shown in Figure 20. The horizontal and vertical flow velocity and the vertical diffusivity show all a decrease during slack tide. This means that the flow will reach into the troughs (1) and the instantaneous circulation will also decrease. The instantaneous circulations are higher compared to the flow over the crests (2), showed by larger arrows. This will be translated to the near-bed velocities, which are already in the process of reversing during the change in ebb and flood tide (3). The horizontal flow velocity show a quicker reverse in direction on the seabed compared to the water column, see Figure 13. This causes a uni-directional transport of the organic matter during slack tide.

The process that causes an increase in organic matter concentration already showed that the bathymetry and the forcing conditions have an influence on the increasing organic matter concentration. Which has also an effect on the transport of the organic matter. Figure 15 showed three peaks during slack tide, which is explained by the transport of organic matter. However, the peaks are lower at $t=9$, which indicates in lower organic matter concentration. The asymmetrical sand wave show an higher increase in concentration on the lee side compared to the stoss side. Which results in a higher concentration transport with ebb tide in the negative x-direction and a lower concentration transport with flood tide in the positive direction.

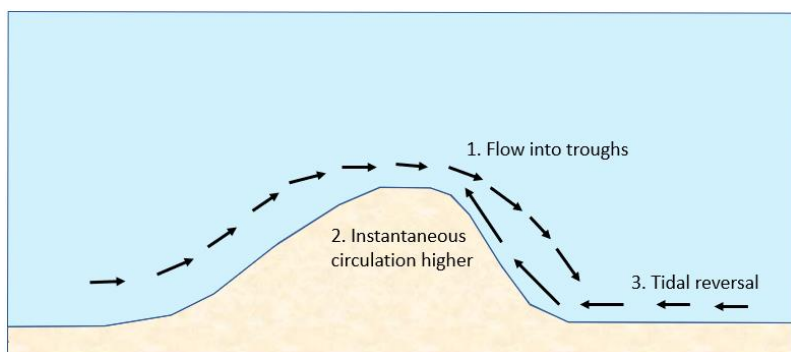


Figure 20 Physical explanation of the transport of organic matter, by showing the tidal reversal from flood to ebb tide.

Discussion

A coupling between the hydro-morphological model and the biogeochemical model has been made for the first time, and the results on the dynamics of organic matter transport are determined. Here the main observations and significance of this finding are discussed.

Organic matter

The one-way coupling shows an increase of organic matter concentration on the lee side during flood tide and on the stoss side during ebb tide for case II - IV. Paragraph 4.5 explained that due to the higher flow velocities, the flow will overshoot the crest, which results in lower velocities in the trough. This also results in an instantaneous circulation behind the sand waves during that period, which ensures the upward flow to the crest. As a result, a weak point develops on the concerning side of the sand wave, depending on the tidal cycle, where the organic matter concentration will increase. A consequence of this is that in the asymmetrical and Texel cases the concentration is higher on the lee side than on the stoss side.

Furthermore, the one-way coupling shows a transport of organic matter during slack tide. Paragraph 4.5 explained that the flow over the crest will decrease, which elevates the instantaneous circulations on stoss or lee side at that time step in the tidal cycle. This will be converted to near-bed velocities, which are already flowing in the other direction. This is why the transport of organic matter occurs in one direction. Furthermore, Figure 15 shows that the transport of organic matter will pass at least three sand waves.

The biogeochemical model produced organic matter at the water surface and will sink in the water columns by the hydrodynamics of the hydro-morphological model. However, in reality the organic matter is already in the water column and is found in the sediment on the seabed. This could mean that the results will be different when this is taken into account.

Organic matter in sediment

The biogeochemical model only used the organic matter in the water column. The organic matter is produced at the water surface and transported by the hydrodynamics obtained from the hydro-morphological model. In reality, organic matter is already in the domain, for example in the sediment itself. Van Kessel et al. (2011) modelled seasonal dynamics of suspended particle matter (SPM) on a sandy seabed, part of which is comprised of organic matter. The algorithm in this study models the seabed into two layers. The first layer can easily resuspended by tidal currents and the second layer may fines entrain and temporarily be stored. This makes a better sediment exchange between the bed layer and the water column. The biogeochemical model could be extended with the help of van Kessel et al. (2011), which results in organic matter both in water column and sediment.

Ecological model

Once the organic matter is also included in the sediment, an ecological model could be then applied. This model would look at the different feeders and the way in which they capture their food. Lessin et al. (2019) showed that both observations and model simulations illustrate differences between deposit and suspension feeders in their rate of activity in response to phytoplankton blooms. The ecological model would ideally be able to predict the locations of the different feeders along the sand waves,

based on the differences in the organisms' ability to capture their food, as well as the concentration and rate of transport of organic matter, both in the sediment and water column.

Erosion and deposition

In the biogeochemical model, erosion and deposition were not taken into account. The coupling only showed the hydrodynamics of the hydro-morphological model coupled with the organic matter in the water column. As a result, the organic matter is neither eroded from nor deposited into the sediment, even though this occurs in reality. There might be several ways to look into the deposition of the organic matter. By using a tracer, one particle of organic matter could be followed from the water surface into the seabed. This would give insights to where and how quickly the organic matter would be deposited, as well as resuspended. Another way could be to turn off all initial conditions on the water surface except for one cell (or only look into organic matter on the crest or trough). The end result would be similar to the tracer modelling to see what happens with the organic matter of one cell in combination with the hydrodynamics.

As already mentioned, the hydro-morphological model uses one grain size, while in the field, the grain size could vary significantly over the sand waves. The trough shows smaller grain sizes compared to the crest and smaller particles will be more easily eroded, relative to the same hydrodynamic conditions. This could also have an influence on the organic matter erosion and deposition in ways in which the current setting (e.g. using single grain size) would not be able to capture.

Hydro-morphological model parameters

The hydro-morphological model in this research is based on the model of van Gerwen et al. (2018). In that study, they mentioned that the model predictions were very sensitive to the model input parameters. Various model parameters have significant influences on the equilibrium wave height and thereby the hydrodynamics and sediment dynamics along the sand waves. The sensitivity of the model outcomes are already done by Krabbendam (2018). This research mentioned that the model is not yet ready for practical application. There are several improvements that could be made, such as including a spatial variable d_{50} (Roos et al., 2007) or changing the boundary conditions based on measurements, including the effect of wind and waves (Campmans et al., 2018). The grain size affects the equilibrium wave height of the sand waves while storm effects decrease the finite sand wave height. This study shows that the bathymetry does have an influence on the hydrodynamics and the distribution of organic matter.

Grid

The grid refinement was also investigated by van Gerwen et al. (2018). Compared to Borsje et al. (2013), a more refined grid was mainly required to accurately describe the long-term evolution towards equilibrium. The grid spacing needs to be small enough to compute small variations in the residual velocity field. The same grid was used in the biogeochemical model, but here no sensitivity analysis has been done yet. This study does not give any errors on the way to implement the same grid together with hydrodynamics in the biogeochemical model. A too small grid could result in organic matter movement that will skip or pass some grid cells, which could give some errors. Too big grid cells could change the accuracy of the results.

Mass balance

In the biogeochemical model the vertical velocities were assumed to be correct and from this, the horizontal velocities were calculated. There was a small, but acceptable, difference between the horizontal velocities from the hydro-morphological model and the calculated velocities in the biogeochemical model, see Figure 6. In the latter case the mass balance needs to be correct. From the hydro-morphological model, this was not the case. The input and the output of each box or cell has to

be equal zero in the biogeochemical model, and the flows or fluxes cannot suddenly be created or eliminated. When the mass balance is not correct the system is not complete and the results will be wrong. The end result would be the model giving a wrong indication of the distribution of the organic matter.

Biogeochemical model parameters

The input values in the biogeochemical model, see Table 3, were based on values from previous experiments and studies at NIOZ. In this research the values were not tested nor was a sensitivity analysis done. There are other possible values that could be used as input, based on the conditions that would be modelled, and the results could be significantly different. For example the settling velocity is an output of the hydro-morphological model and can be used instead of the sinking rate in the biogeochemical model.

Field campaign

The coupling between the models has also not yet been validated with field data. This research makes an initial step by implementing the field data from the Texel field campaign into the model. From the case IV scenario, the simulated conditions were more represented of the field which makes it easier and perhaps more accurate for comparing with the Texel field data (i.e., collected samples and measurements). At this moment the results match well with the field measurements of Cheng et al., (submitted) and Damveld et al. (2018). Furthermore, the sand waves in the Texel case are not in equilibrium, which means that the hydrodynamics are not in balance with the sea bed.

Two-way coupling

This research made an attempt to couple the hydro-morphological model with the biogeochemical model, through a one-way coupling. This was done by using the outputs from the hydro-morphological model in Delft3D (the hydrodynamics) in the biogeochemical model. The one-way coupling clearly showed the consequences of the hydrodynamics on the distribution of the organic matter. However, the model could be further developed by including additional parameters to further investigate the interactions between sand wave dynamics and benthic organisms. Moreover, the effects of the benthic organisms on the sand wave dynamics should also be considered. But in order to achieve this, the model needs a back coupling or a two-way coupling (e.g. Damveld et al., 2019; Maris, 2018). This two-way coupling could be done by taking the bed-roughness for example.

Suspended sediment concentration

The study of Borsje et al. (2014) showed higher tide-averaged suspended sediment concentrations on the crest compared to the trough. Here other dimensions are used for the sand wave, but the grain size of 0.35 mm is the same as in this research. Furthermore, Maris (2018) used the suspended sediment concentration as available food for the worms. This is in contrast to the results of the biogeochemical model, which shows higher organic matter concentration between trough and flanks. However, the organic matter concentration is a closer prediction to the food supply of the benthic organisms, and corresponds better with the field measurements.

Transport of organic matter

The results show a difference in transport of organic matter over the asymmetrical sand waves. The increase in organic matter concentration is higher on the lee side during flood tide compared to the stoss side during ebb tide. This means that a higher organic matter concentration will be transported in the negative x-direction. The consequences of this is not investigated in this research.

Conclusion and recommendations

6.1 Conclusion

This section will address the research questions as stated in paragraph 1.3. The research objective was formulated as follows:

To develop a tool to model the distribution of organic matter over sand waves by coupling the hydro-morphological model with the biogeochemical model, and to analyse the effect of bathymetry and forcing conditions.

The answers are given for each question.

How do the hydrodynamics fluctuate along a flat bed, a symmetrical and an asymmetrical sand wave?

The hydrodynamics that were used in this research were the horizontal and vertical flow velocity and the vertical diffusivity. These were investigated for four cases and three types of bed forms: a flat bed, a symmetrical sand wave and an asymmetrical sand wave. The results showed that the difference in bed forms has a measurable influence on the hydrodynamics. The tide-averaged flow velocity for the flat bed case is zero everywhere, and there is no perturbations in the bed and the tide is symmetrical. The symmetrical sand wave, on the other hand, illustrated tide-averaged circulations on both sides of the sand waves. Then, the asymmetrical and the Texel sand wave showed only a tide-averaged circulation on the lee side of the sand wave. This was due to the asymmetry of the sand wave and the residual current, which caused a net flow in the same direction as the flood tide.

The near-bed velocity further illustrated a difference in velocity on the lee and stoss sides during ebb and flood tide for cases II - IV. During flood tide the flow is higher on the stoss side, compared to the lee side. Whereas the opposite holds true for during ebb tide, and lower velocities were found on the stoss side and higher velocities on the lee side.

The vertical flow velocity similarly showed a difference between the symmetrical and asymmetrical sand waves on the stoss and lee sides, because of differences in bathymetry. The symmetrical sand wave produced the same vertical flow velocities on both sides during ebb and flood tide. In contrast, the asymmetrical sand wave had much higher vertical velocities on the lee side at flood tide and lower vertical flow velocities on the stoss side during ebb tide. This means that the bathymetry does have an influence on the vertical velocity. The steeper the slope of the sand wave, the higher the vertical flow velocity. Furthermore, the differences in the vertical flow velocities could indicate the presence of flow circulations.

The bathymetry also had an influence on the vertical diffusivity as well, where all diffusivities were higher compared to the flat bed case. Comparing the diffusivities with the flow, both showed the highest values during ebb and flood tide, but the vertical diffusivities had the lowest values a short while after slack tide (i.e., small time lag).

Another interesting observation was the change in tides. In all four cases, the results showed a quicker change from ebb to flood and vis versa at the seabed versus at the water surface.

Generally, during flood tide, the flow will accelerate on the stoss side. This causes a downward movement of the vertical flow velocities. Afterwards, the flow will overshoot the crest, which causes lower flow velocities on the lee side, and consequently, instantaneous circulations and an upward movement of the vertical flow velocities. During ebb tide the reverse occurs. Because of the asymmetry in the sand wave and the residual current of the asymmetrical sand waves, the acceleration was less on the stoss side and the instantaneous circulation was higher on the lee side during flood tide.

What is the effect of the bathymetry of the sand waves and forcing conditions on the distribution of organic matter in the water column?

The results of the one-way coupling between the hydro-morphological model and the biogeochemical model clearly illustrated two behaviours: the increase in organic matter concentration during flood and ebb tide and the transport of organic matter during slack tide.

The tide-averaged organic matter concentration was higher on both sides of the symmetrical sand wave (depending on flood and ebb tide) and only on the lee side of the asymmetrical sand wave. This shows already the effect of the bathymetry of the sand waves and forcing conditions for tide-averaged organic matter concentration. The tide-averaged circulation on the lee side in the asymmetrical case is the same idea for the increase in organic matter concentration. During ebb and flood tide the flow will accelerate on the flanks of the sand waves, because of the decrease in water depth. Subsequently, the flow will overshoot the crest which occurs in lower velocities on one of the flanks and in the troughs depending on the tidal cycle. In the ensuing instantaneous circulation, flow is then directed to the crest (which is showed by the vertical flow velocities). This causes a weak point on the stoss/lee side, depending on ebb or flood tide, where the organic matter show an increase in concentration. The asymmetrical case has a larger stoss length and a shorter lee length, but almost the same sand wave height. This means that the instantaneous circulation is higher on the lee side and smaller (or not existing) on the stoss side and results in a larger increase in concentration on the lee side compared to the stoss side.

The second behaviour is the disturbance to the increasing organic matter concentration process. When the flow decreases during slack tide, it will reach into the troughs. The instantaneous circulations are higher compared to the flows over the crests. This will be translated to the near-bed velocities, which are already in the process of reversing during the change in ebb and flood tide. Consequently, this causes a uni-directional transport of the organic matter during slack tide. The results show that the transport occurs over at least three sand waves. After the transport, the organic matter shows an increase in concentration on the other side of the sand wave. Furthermore, the first behaviour showed that the bathymetry and the forcing conditions have an influence on the increasing organic matter concentration. This means that the bathymetry and the forcing conditions have also an effect on the transport. The asymmetrical sand wave show an higher increase in concentration on the lee side compared to the stoss side. Which results in a higher concentration transport during ebb tide in the negative x-direction and a lower concentration transport during flood tide in the positive x-direction.

The four cases in this research differ in bathymetry and forcing conditions, e.g. type of tide and residual currents. This clearly has an influence on the distribution of organic matter. Case II, III and IV all showed a wider range in organic matter concentrations than the flat bed case (case I). The symmetrical sand waves had the same organic matter concentration on both sides. On the other hand, the asymmetrical sand waves (case III) had a higher concentration on the lee side compared to the stoss side. The same result was repeated in the Texel case. Here the wave height of the sand waves also affected the concentration as well, with the smaller wave heights showing lower concentrations.

6.2 Recommendations

This section gives some recommendations with regard to this research.

Water column

In the biogeochemical model the organic matter is produced at the water surface and is only distributed in the water column. In reality the organic matter is in the sediment itself for example. This means that the biogeochemical model could be extended for a better view on the transport of organic matter along the sand waves, as discussed in the discussion section.

Organic matter

This study make use of organic matter as food supply for benthic organisms. The organic matter could provide an preliminary prediction on the distribution of the benthic organisms along the sand waves. However, this study does not look into the different benthic organisms. Lessin et al. (2019) showed that both observations and model simulations illustrate differences between deposit and suspension feeders in their rate of activity in response to phytoplankton blooms. The biogeochemical model could be extended based on the differences in the organisms' ability to capture their food, as well as the concentration and rate of transport of organic matter, both in the sediment and water column. Then the biogeochemical model becomes an ecological model and is able to predict the location of the different feeders along the sand waves.

Two-way coupling

This study made a one-way coupling between the hydro-morphological model and the biogeochemical model. However, the sand wave dynamics have an effect on the habitat of the benthic organisms and the benthic organisms have an effect on the migration of the sand waves. To investigate the affection of the sand wave dynamics and the benthic organism on each other, the models need a two-way coupling.

References

- Baptist, M. J., van Dalen, J., Weber, A., Passchier, S., & van Heteren, S. (2006). The distribution of macrozoobenthos in the southern North Sea in relation to meso-scale bedforms. *Estuarine, Coastal and Shelf Science*, 68(3–4), 538–546. <https://doi.org/10.1016/j.ecss.2006.02.023>
- Besio, G., Blondeaux, P., Brocchini, M., Hulscher, S. J. M. H., Idier, D., Knaapen, M. A. F., ... Vittori, G. (2008). The morphodynamics of tidal sand waves: A model overview. *Coastal Engineering*, 55(7–8), 657–670. <https://doi.org/10.1016/j.coastaleng.2007.11.004>
- Besio, G., Blondeaux, P., Brocchini, M., & Vittori, G. (2004). On the modeling of sand wave migration. *Journal of Geophysical Research C: Oceans*, 109(4). <https://doi.org/10.1029/2002JC001622>
- Besio, G., Blondeaux, P., & Vittori, G. (2006). On the formation of sand waves and sand banks. *J. Fluid Mech.*, 557, 1–27. <https://doi.org/10.1017/S0022112006009256>
- Bianchi, T. S. (2011). The role of terrestrially derived organic carbon in the coastal ocean: A changing paradigm and the priming effect. *PNAS*, 108(49), 19473–19481. <https://doi.org/10.1073/pnas.1017982108>
- Borsje, B. W., Hulscher, S. J. M. H., Herman, P. M. J., & de Vries, M. B. (2009). On the parameterization of biological influences on offshore sand wave dynamics. *Ocean Dynamics*, 59, 659–670. <https://doi.org/10.1007/s10236-009-0199-0>
- Borsje, B. W., Kranenburg, W. M., Roos, P. C., Matthieu, J., & Hulscher, S. J. M. H. (2014). The role of suspended load transport in the occurrence of tidal sand waves. *Journal of Geophysical Research: Earth Surface*, 119(4), 701–716. <https://doi.org/10.1002/2013JF002828>
- Borsje, B. W., Roos, P. C., Kranenburg, W. M., & Hulscher, S. J. M. H. (2013). Modeling tidal sand wave formation in a numerical shallow water model: The role of turbulence formulation. *Continental Shelf Research*, 60, 17–27. <https://doi.org/10.1016/j.csr.2013.04.023>
- Borsje, B. W., Vries, M. B. De, Bouma, T. J., Besio, G., Hulscher, S. J. M. H., & Herman, P. M. J. (2009). Modeling bio-geomorphological influences for offshore sandwaves. *Continental Shelf Research*, 29, 1289–1301. <https://doi.org/10.1016/j.csr.2009.02.008>
- Burchard, H., Craig, P. D., Gemmrich, J. R., Haren, H. V., Mathieu, P., Meier, H. E. , ... Wijesekera, H. W. (2008). Observational and numerical modeling methods for quantifying coastal ocean turbulence and mixing. *Progress in Oceanography*, 76, 399–442. <https://doi.org/10.1016/j.pocean.2007.09.005>
- Campmans, G. H. P., Roos, P. C., de Vriend, H. J., & Hulscher, S. J. M. H. (2018). The Influence of Storms on Sand Wave Evolution : A Nonlinear Idealized Modeling Approach. *Journal of Geophysical Research: Earth Surface*. <https://doi.org/10.1029/2018JF004616>
- Cheng, C. H., Soetaert, K., & Borsje, B. W. (2017). Sediment sorting over asymmetrical tidal sand waves. *Submitted*.
- Damen, J. M., van Dijk, T. A. G. P., & Hulscher, S. J. M. H. (2018). Spatially Varying Environmental Properties Controlling Observed Sand Wave Morphology. *Journal of Geophysical Research: Earth Surface*, 123(2), 262–280. <https://doi.org/10.1002/2017JF004322>
- Damveld, J. H., Reijden, K. J. Van Der, Cheng, C., Koop, L., Haaksma, L. R., Walsh, C. A. J., ... Hulscher, S. J. M. H. (2018). Video Transects Reveal That Tidal Sand Waves Affect the Spatial Distribution

- of Benthic Organisms and Sand Ripples. *Geophysical Research Letters*, 45(11), 837–846.
<https://doi.org/10.1029/2018GL079858>
- Damveld, J. H., Roos, P. C., Borsje, B. W., & Hulscher, S. J. M. H. (2019). Modelling the two-way coupling of tidal sand waves and benthic organisms: a linear stability approach. *Environmental Fluid Mechanics*2.
- De Jong, M. F., Baptist, M. J., Lindeboom, H. J., & Hoekstra, P. (2015). Relationships between macrozoobenthos and habitat characteristics in an intensively used area of the Dutch coastal zone. *ICES Journal of Marine Science*, 72, 2409–2422.
- Dodd, N., Blondeaux, P., Calvete, D., de Swart, H. E., Falques, A., Hulscher, S. J. M. H., ... Vittori, G. (2003). Understanding coastal morphodynamics using stability methods. *Journal of Coastal Research*, 19(4), 849–865.
- Hulscher, S. J. M. H. (1996). Tidal-induced large-scale regular bed form patterns in a three-dimensional shallow water model. *Journal of Geophysical Research*, 101(C9), 20,727–20,744.
- Janssen, F., Cardenas, M. B., Sawyer, A. H., Dammrich, T., Krietsch, J., & de Beer, D. (2012). A comparative experimental and multiphysics computational fluid dynamics study of coupled surface – subsurface flow in bed forms. *Water Resource Research*, 48, 1–16.
<https://doi.org/10.1029/2012WR011982>
- Knaapen, M. A. F. (2005). Sandwave migration predictor based on shape information. *Journal of Geophysical Research*, 110(4), 1–9. <https://doi.org/10.1029/2004JF000195>
- Krabbendam, J. (2018). Modelling the long term evolution of observed tidal sand waves in the North Sea. *MSc Thesis*.
- Lesser, G. R., Roelvink, J. A., van Kester, J. A. T. M., & Stelling, G. S. (2004). Development and validation of a three-dimensional morphological model. *Coastal Engineering*, 51(8–9), 883–915.
<https://doi.org/10.1016/j.coastaleng.2004.07.014>
- Lessin, G., Bruggeman, J., Mcneill, C. L., & Widdicombe, S. (2019). Time Scales of Benthic Macrofaunal Response to Pelagic Production Differ Between Major Feeding Groups. *Frontiers in Marine Science*, 6(January), 1–12. <https://doi.org/10.3389/fmars.2019.00015>
- Maris, H. L. (2018). Modeling the two-way coupling between *Lanice Conchilega* and sand waves on the bottom of the North Sea. *MSc Thesis*.
- Németh, A. A., Hulscher, S. J. M. H., & de Vriend, H. J. (2003). Offshore sand wave dynamics, engineering problems and future solutions. *Pipeline and Gas Journal*.
- Németh, A. A., Hulscher, S. J. M. H., & De Vriend, H. J. (2002). Modelling sand wave migration in shallow shelf seas. *Continental Shelf Research*, 22(18–19), 2795–2806.
[https://doi.org/10.1016/S0278-4343\(02\)00127-9](https://doi.org/10.1016/S0278-4343(02)00127-9)
- NIOZ. (n.d.). Retrieved January 28, 2019, from <https://www.nioz.nl/en/about>
- R. Core Team. R: A Language and Environment for Statistical Computing. R Foundation for Statistical Computing, Vienna, Austria URL <http://www.R-project.org/> (2014).
- Rodi, W. (1980). Turbulence models and their application in hydraulics- a state of the art review. *University of Karlsruhe, Karlsruhe, Germany*.
- Roos, P. C., Hulscher, S. J. M. H., van der Meer, F., van Dijk, T. A. G. P., Wientjes, I. G. M., & van den Berg, J. (2007). Grain size sorting over offshore sandwaves : Observations and modelling. *5th IAHR Symposium on River, Coastal and Estuarine Morphodynamics, RCEM 2007*, (Hirano 1971),

649–656.

- Shimeta, J. (2009). Influence of flow speed on the functional response of a passive suspension feeder, the spionid polychaete *Polydora cornuta*. *Marine Biology*, *156*, 2451–2460. <https://doi.org/10.1007/s00227-009-1270-6>
- Soetaert, K., & Herman, P. M. J. (2009). *A Practical Guide to Ecological Modelling*.
- Soetaert, K., Herman, P. M. J., & Middelburg, J. J. (1996). Dynamic response of deep-sea sediments to seasonal variations : A model. *Limnol. Oceanogr.*, *41*(8), 1651–1668.
- Soetaert, K., Mohn, C., Rengstorf, A., Grehan, A., & Van Oevelen, D. (2016). Ecosystem engineering creates a direct nutritional link between 600-m deep cold-water coral mounds and surface productivity. *Scientific Reports*, *6*(April), 1–9. <https://doi.org/10.1038/srep35057>
- Soetaert, K., & Petzoldt, T. (2010). Solving Differential Equations in R : Package deSolve. *Journal of Statistical Software*, *33*(9).
- Terwindt, J. H. J. (1971). Sand waves in the southern bight of the North Sea. *Marine Geology*, *10*(1), 51–67. [https://doi.org/10.1016/0025-3227\(71\)90076-4](https://doi.org/10.1016/0025-3227(71)90076-4)
- Tonnon, P. K., van Rijn, L. C., & Walstra, D. J. R. (2007). The morphodynamic modelling of tidal sand waves on the shoreface. *Coastal Engineering*, *54*(4), 279–296. <https://doi.org/10.1016/j.coastaleng.2006.08.005>
- van Gerwen, W., Borsje, B. W., Damveld, J. H., & Hulscher, S. J. M. H. (2018). Modelling the effect of suspended load transport and tidal asymmetry on the equilibrium tidal sand wave height. *Coastal Engineering*, *136*(March 2017), 56–64. <https://doi.org/10.1016/j.coastaleng.2018.01.006>
- van Kessel, T., Winterwerp, H., van Prooijen, B., & Borst, W. (2011). Modelling the seasonal dynamics of SPM with a simple algorithm for the buffering of fines in a sandy seabed. *Continental Shelf Research*, *31*, s124–s134.
- van Nugteren, P., Moodley, L., Brummer, G., Heip, C. H. R., Herman, P. M. J., & Middelburg, J. J. (2009). Seafloor ecosystem functioning : the importance of organic matter priming. *Marine Biology*, 2277–2287. <https://doi.org/10.1007/s00227-009-1255-5>
- Widdows, J., & Brinsley, M. (2002). Impact of biotic and abiotic processes on sediment dynamics and the consequences to the structure and functioning of the intertidal zone. *Journal of Sea Research*, *48*(2), 143–156. [https://doi.org/10.1016/S1385-1101\(02\)00148-X](https://doi.org/10.1016/S1385-1101(02)00148-X)